United Nations ECE/TRANS/WP.5/GE.3/2019/9

Economic and Social Council

Distr.: General
13 February 2019

Original: English

Economic Commission for Europe

Inland Transport Committee

Working Party on Transport Trends and Economics

Group of Experts on Climate Change Impacts and Adaptation for Transport Networks and Nodes

Seventeenth session
Geneva, 24 and 25 April 2019
Item 4 of the provisional agenda
Discussions on the final report of the Group of Experts

Climate Variability and Change: Trends and Projections*

Submitted by a consultant

I. Introduction

1. This document presents a review of the recent trends and variability of different climatic factors that can affect transportation together with a review of the recent projections on the evolution of these factors in the twenty-first century. The Group of Experts requested at the sixteenth session that this case study is tabled as on official document at the seventeenth session.

II. Climate Variability and Change[1]: Recent Trends and Projections

2. The information presented here focuses on climatic factors and hazards the variability and change of which can impact transportation networks in the ECE region; these include the temperature, precipitation (rainfall), snow, ice and sea level as well as the

* The present document contains the text submitted to the secretariat reproduced without any changes.

[1] Note that Climate Variability and Change (CV & C) refers to the variability and sustained change of climatic conditions relative to a reference period, e.g. the pre-industrial times or periods during which the infrastructure used today was constructed (e.g. 1961–1990, 1986–2005 or 1981–2010).

extreme events (cross document reference to be added). Information on these climatic factors until 2013 has been presented in a previous ECE report (ECE, 2013). In the present report, focus is placed on their recent trends and projections.

3. There is overwhelming evidence for a warming world since the 1850s in many environments (from the upper atmosphere to the ocean deeps). In most cases, however, discussions on Climate Variability and Change (CV & C) focus on the land surface temperature rise, which is just one of the indicators of changing climate, with others being the changes in e.g. the atmospheric and oceanic temperatures, sea level, precipitation, and glacier, snow and sea ice covers (Fig. 1). Generally, the now better recorded and understood climate dynamics suggest a substantial and, in some cases, accelerating climatic change. It appears that the various climatic hazards for the transportation infrastructure and operations (ECE, 2013) will deteriorate.

Figure 1

Change of climatic factors. Each line represents an independently derived estimate. In each panel all data sets have been normalized to a common period of record (IPCC, 2013)

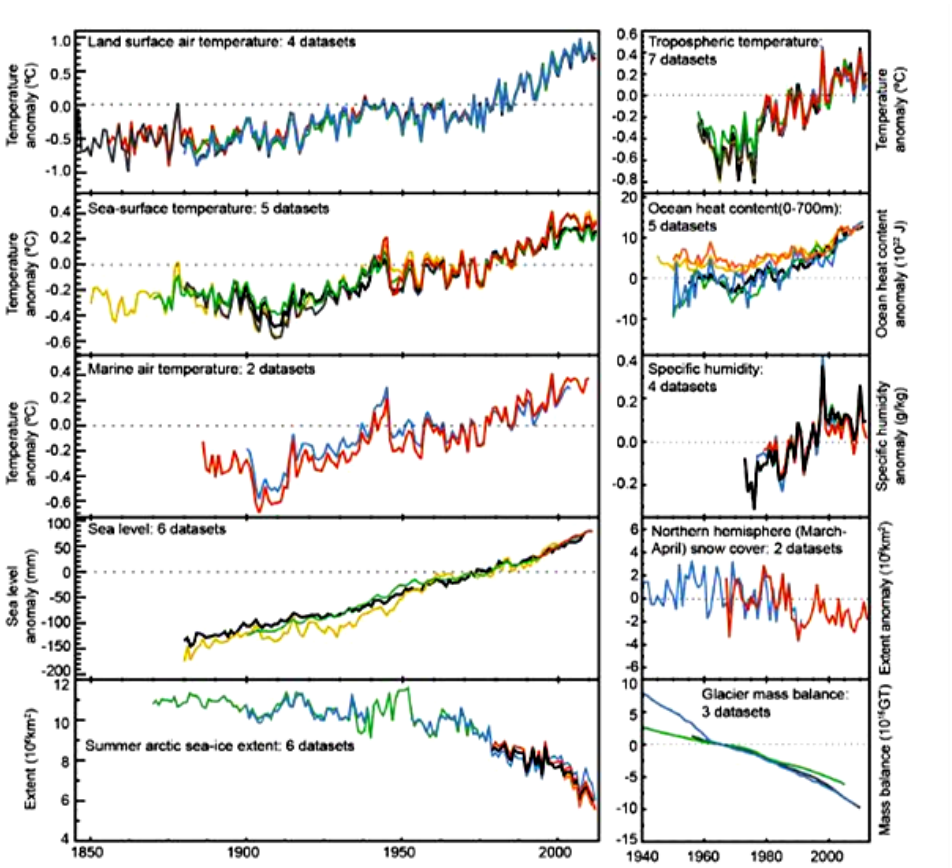

A. Temperature

1. Trends

4. Temperature appears to be increasing in many components of the earth system (Fig. 1). Globally-averaged, near-surface temperature change is a most cited indicator of CV & C, as it is directly related to both the climate change causes, i.e. the increase in

cumulative Greenhouse Gas-GHG emissions (IPCC, 2013) and the planetary energy balance (Fourier 1827), and many impacts and risks (Arnell et al., 2014). Although each year (or decade) has not been always warmer than the previous, there has been certainly a warming trend in recent decades (Fig. 2).

Figure 2

Global mean temperature anomalies, with respect to the 1850–1900 baseline, for the five global datasets (Source: UK Met Office Hadley Centre). In the individual datasets, 2017 was second warmest in the re-analysis datasets ERA-Interim and JRA-55 (WMO, 2018)

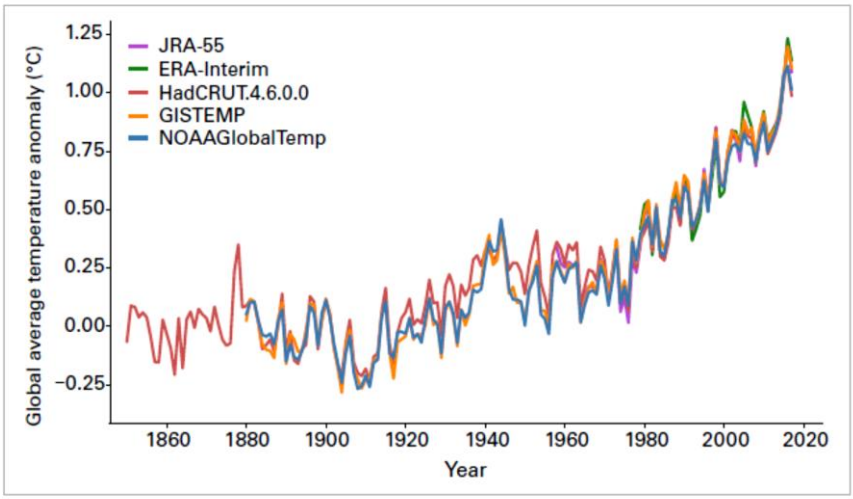

5. Warming of the climate system is indisputable. All observations suggest increases in the globally averaged surface temperatures, most likely as a result of the increasing atmospheric GHG concentrations (IPCC, 2007; 2013). The five-year mean temperature in 2013–2017 (Fig. 3), which gives a longer-term perspective on the evolving temperatures, has been 0.4°C above the 1981–2010 average and 1.0°C above pre-industrial values; it is the highest on record. Annual mean temperatures are also influenced by various climatic modulations and particularly the El Niño-Southern Oscillation (ENSO). El Niño years are warmer than the neutral or La Niña years.

6. A strong El –Nino event developed in 2015–2016. 2016 has been the warmest year on record, with the globally-averaged temperature being about 1.1°C above the pre-industrial time (NOAA, 2017a). Record temperatures were widespread in the Northern Hemisphere (NH) (NSIDC, 2017), with the global temperature in early 2016 being about 1.5°C above that recorded in the early industrial revolution (Simmons et al., 2017).[2] A vast Eurasian region as well as Alaska showed temperatures in February more than 5°C above the 1981–2010 average. Sea surface temperature (SST) was also the warmest on record (NOAA, 2016). 2015, which was affected by the El Nino only at its later part, showed also record temperatures, being the second warmest year on record. By comparison, the El Niño neutral years 2014 and 2017 recorded near surface land temperatures of 0.88°C ± 0.2°C higher than the 1961–1990 average (WMO, 2014) and 1.31°C above the twentieth century average, respectively.[3] 2017 was the warmest non-El Niño year on record (and the third

[2] An alarming development in view of the 2015 Paris Agreement the aim of which is to 'hold' the global average temperature increase to well below 2°C above pre-industrial levels (UNFCCC, 2015, IPCC, 2018).

[3] See also www.ncdc.noaa.gov/sotc/global/201713

warmest overall), whereas the also weak La Niña year 2018 and the neutral 2014 were the fourth and fifth warmest years on record, respectively (NASA, 2016, NOAA, 2017b; WMO, 2018). The evidence is consistent with a steady warming trend since the 1970s, superimposed on random, stationary, short-term variability (Rahmstorf et al., 2017). Regarding the ECE region, recently there has been a clear warming trend over most of its areas (Fig. 3).

Figure 3

Average global temperature 2013-2017, as compared to the average of 1951 – 1980 (left) (NASA Goddard Institute for Space Studies, climate.nasa.gov/news/2671/long-term-warming-trend-continued-in-2017-nasa-noaa/) (left); and land and ocean departure temperature anomalies in 2018 compared to the 1981–2010 average (right)

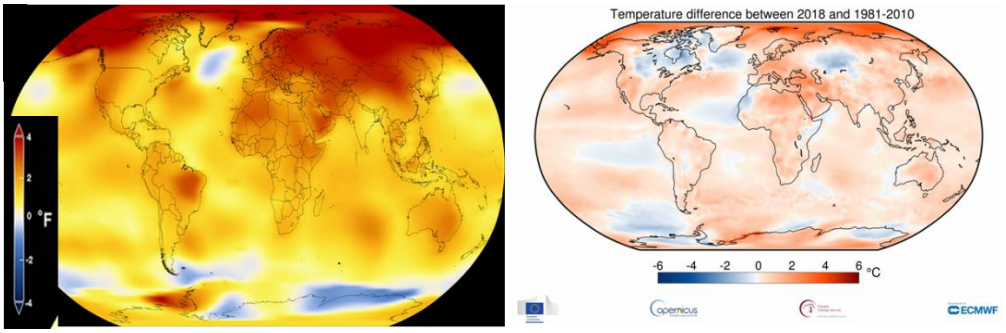

7. In 2003–2013 there was an apparent slowdown in the rate of the global mean (surface) temperature rise (Fig. 2) compared to climate model projections (Dieng et al., 2017a). This slowdown ('the global warming hiatus') has been attributed to uncertainties in the dataset biases and processes related to 'external' forcing, such as volcanic eruptions, stratospheric changes in water vapor and industrial aerosols, ocean heat redistribution, solar activity and the ocean cycle variability (IPCC, 2013; MetOffice, 2014; Cowtan and Way, 2014; Karl et al, 2015; Fyfe et al., 2016; Yan et al., 2016; Cheng et al., 2019).

8. Climate is controlled by the heat inflow and outflow and its storage dynamics (IPCC, 2013). Most of the heat storage occurs in the ocean which absorbs most of the heat added to the system (Cheng et al., 2019a). In recent decades, there has been evidence of an increasing ocean heat content, with the rate being estimated as 0.50–0.65 Wm-2 for the period 2003–2013 (Dieng et al., 2017a). The past 5 years (2014–1018) have been the warmest on record for the upper ocean (Cheng et al., 2019b).

2. Projections

9. The atmospheric temperature has been projected to increase by 1.0°C–3.7°C (mean estimates) in the end of the twenty-first century, depending on the GHG concentration scenario.[4] The ocean will also warm (IPCC, 2013). The strongest surface warming is projected for the subtropics and tropics, whereas warming at greater depths will be more pronounced in the Southern Ocean. By 2100, warming of the upper 100 m of the ocean is expected to be between 0.6°C (RCP2.6) and 2.0°C (RCP8.5), and in the upper 1,000 m between 0.3 °C (RCP2.6) and 0.6°C (RCP8.5). For RCP4.5, half of the energy taken up by the ocean will be stored in the uppermost 700 m and 85 per cent in the uppermost 2000 m (e.g. Cheng et al., 2019a; 2019b).

[4] Since the last IPCC Assessment Report AR5 (2013) forecasts are made on the basis of the Representative Concentration Pathways-RCP scenarios and not the previously used IPCC SRES scenarios. The CO2 equivalent concentrations have been set to: RCP 8.5, 1370 C02-equivalent in 2100; RCP 6.0 850 CO2-equivalent in 2100; RCP 4.5, 650 CO2-equivalent in 2100; and RCP 2.6, peak at 490 CO2-equivalent before 2100 (Moss et al., 2010).

Figure 4

Projected changes in annual (left), summer (middle) and winter (right) surface air temperature (°C) in 2071 - 2100 compared to 1971 - 2000 for forcing scenarios RCP4.5 (top) and RCP8.5 (bottom). Model simulations are from RCMs (EURO-CORDEX initiative) (EEA, 2014a)

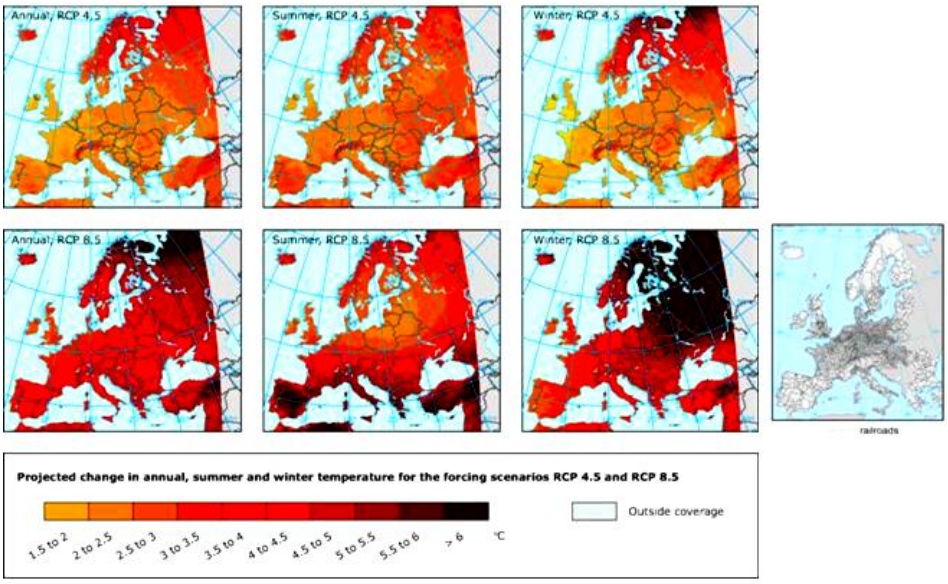

10. Climate does not and will not change uniformly. Temperatures rise faster close to the poles than at the equator (e.g. Fig. 3). A recent IPPC report (IPCC, 2018) projects significant regional climatic differences between the present-day conditions and those under a global warming of 1.5°C and 1.5°C–2°C above the pre-industrial times, including increases in the hot extremes in most inhabited regions (high confidence). Under all scenarios, large temperature increases have been projected by global models over the ECE region, particularly for its northern areas (IPCC, 2013). Regional models also suggest very significant warming for Europe (Fig. 4), particularly under the RCP8.5 scenario. Northeastern Europe as well as the Mediterranean region will be the worst hit, with significant implications for the ECE transportation networks.

11. Vogel et al. (2017) have found (using simulations by CTL and SM20c models) that the daily maximum temperature (TXX) will also increase until the end of the century. Projected changes are more pronounced in the CTL simulations than the SM20c simulations, with regional increases of up to 10°C and 6°C, respectively.

B. Precipitation

1. Trends

12. Global land rainfall data show an increasing trend, especially in middle and high latitudes (low confidence before 1951, medium confidence afterwards) (EPA, 2015). When only the mid-latitudes in the Northern Hemisphere (NH) are considered, confidence in the post-1951 trends become high. In the periods 1931–1960 and 1941–1970, there were larger differences compared to those in the 1951–2000 period; more rainfall occurred over W. Africa and less over the SE Asia and Indonesia (Meyer-Christoffer et al., 2015). Schneider et al. (2017) applied mean weather-dependent corrections to precipitation data from 75,100 meteorological stations (Global Precipitation Climatology Center-GPCC) and found a mean annual precipitation of about 855 mm (excluding Antarctica) for the period 1951–2000;

they also suggested that a warming of about 1°C relative to pre-industrial time can result to a 2–3 per cent increase in global precipitation.

13. In recent years, land precipitation has been strongly influenced by the El Niño-Southern Oscillation (ENSO). The recent 6–year period followed a strong La Niña year (2011 – early 2012) that produced very wet conditions; 2011 was assessed by NOAA as the second-wettest year on record. However, 2013 and 2014 were close to the long-term average. The western US, eastern Australia and Brazil had large areas where rainfall in October 2012 – September 2015 was below the 10th percentile, whereas there were also regions where precipitation exceeded the 90th percentile (e.g. in eastern Russia). In Europe there was a marked north/south split, with wet conditions in Scandinavia and dry conditions in much of the central and southeastern Europe. In 2014, very dry conditions occurred also over much of the central US and the central and western Russian Federation (WMO, 2014; Met Office 2014).

14. In 2016, global precipitation was influenced by the transition from the El Niño conditions in the early year to the neutral or weak La Niña conditions in the second half of the year; this resulted in seasonal contrasts in many regions. Precipitation above the 90th percentile was observed in a large swath of the ECE region extending from Kazakhstan across the western Russian Federation into Finland, northern Sweden and Norway. However, large areas of the northern/central Russian Federation were dry, with much of the region between the Urals and Lake Baikal and to the north of 55 °N having precipitation below the 10th percentile. Annual precipitation was close to average over most of central and western Europe, but with a very wet first half and a dry second half of the year. Belgium is a particular example of such variability; some of its areas had their wettest January–June period on record (62 per cent above average), followed by the third-driest July–December period on record (36 per cent below average) (WMO, 2017). Another non-typical example has been California, where the seasonal rainfall was near average (after 4 very dry years), increasing towards the end of 2016. In 2017, there were fewer areas with large precipitation anomalies than there had been in the previous years, as the influence of the strong 2015–2016 El Niño ended (WMO, 2018).

2. Projections

15. Precipitation is expected to change in an even more complex manner than temperature. Heavy precipitation has been projected for some regions (medium confidence), with droughts and precipitation deficits expected in other regions (medium confidence) (IPCC, 2013; 2018). Changes in precipitation patterns are projected for the European part of the ECE region, with the north generally becoming wetter and the south drier (Fig. 5).

Figure 5

Projected change of daily precipitation in winter (left) and summer (right), at the end of the century (2071–2100) compared to the present climate (1981-2010), under RCP8.5

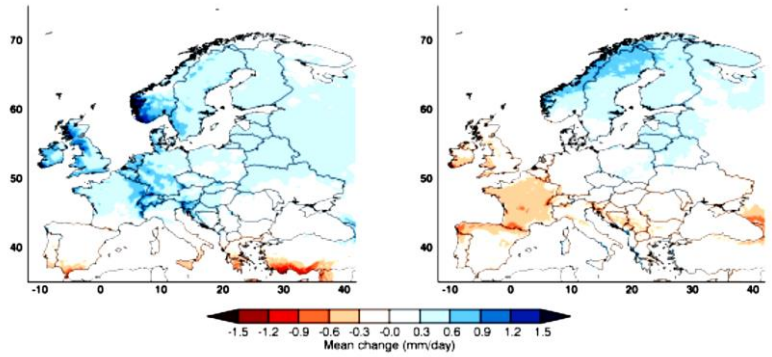

16. At the same time, although summers may become (overall) drier, downpours could become heavier. In the UK, for instance, simulations indicate that intense downpours that may generate flash floods (> 30 mm in an hour) could become almost 5 times more frequent by 2100 (MetOffice, 2014). Widespread droughts have been also projected for most of southwestern N. America for the mid to late twenty-first century; by comparison, central Europe, the Mediterranean and parts of N. America are projected to show less long and intense droughts (Milly et al., 2008; IPCC, 2013; Dai, 2013; IPCC, 2018).

C. Snow, sea ice and permafrost

1. Trends

17. The cryosphere component of the Earth system includes solid precipitation, snow cover, sea ice, lake and river ice, glaciers, ice caps, ice sheets, permafrost and the seasonally frozen ground. The elements for which a brief assessment is provided here include the snow cover, sea ice, glaciers and ice sheets and the permafrost. Assessments of their current state/trends and future evolution are particularly important for transportation in the Arctic ECE regions (for e.g. the Russian Federation, Canada and the USA).

18. The spring snow cover extent (SCE) has decreased across the NH since the 1950s (IPCC, 2013; NSIDC, 2017). SCE in the NH (about the 98 per cent of the global snow cover) has declined by 11.7 per cent per decade in June (EEA, 2015a) over the period 1967 - 2012. However, the trend is not uniform. Some regions (e.g. the Alps and Scandinavia) showed consistent decreases in their snow cover depth at low elevations but increases at high elevations, whereas in other regions (e.g. the Carpathians, Pyrenees, and Caucasus) there were no consistent trends (EEA, 2012).

19. Despite the overall high temperatures of the most recent period, there were still episodes of abnormal cold and snow. A prolonged period of extreme cold affected the central and western Europe in early 2012, the worst cold spell since 1987. The winters of 2013–2014 and 2014–2015 were also significantly colder than normal in the central and eastern USA and the southern Canada, with persistent low temperatures for extended periods; in February 2015, temperatures in Montreal, Toronto and Syracuse did not rise above 0°C. There were also frequent coastal snowfalls, with Boston experiencing its highest seasonal snowfall on record (WMO, 2016). In 2016, mean annual snow cover extent (SCE) in the NH was 24.6 million km2, 0.5 million km2 below the 1967–2015 average, despite the large January snow storms in N. America (e.g. NOAA, 2017a). In Eurasia, the winter SCE was 270,000 km2 below average (WMO, 2017). However, the 2017 SCE in NH was close or above the 1981–2010 average for most of the year, particularly in northwestern Russia and Scandinavia (WMO, 2018).

20. Arctic sea ice is in decline (Figs. 1 and 6). Arctic sea ice usually expands during the cold season to a March-April maximum, and then contracts during the warm season to a September minimum. In contrast, Antarctic sea ice shows its minimum extent in February-March and expands during the South Hemisphere (SH) cold season to a September maximum. Minimum Arctic sea ice extent has declined by about 40 per cent since 1979 with the most records in ice minima having occurred in the last decade (NOAA, 2017a).

21. Arctic sea-ice extent (SIE) was at record low levels for much of 2016 (WMO, 2017). The seasonal maximum of 14.52 million km2 (24th March) was the lowest in the satellite record; notable exceptions were observed in the Labrador Sea, and the Baffin and Hudson Bays. Arctic maximum and minimum SIEs were 1.12 and 2.08 million km2 below the 1981-2010 average, respectively. Antarctic SIE was close to the 1979 – 2015 average for

the first 8 months of 2016, reaching a seasonal maximum of 18.44 million km2. However, following an exceptionally rapid spring melt, the November SIE was 14.54 million km2 (the lowest on record). The reasons behind the Antarctic SIE collapse in late 2016 are not yet understood, having been described as a "black swan" event (NSIDC, 2017). In 2017, SIE was well below the 1981–2010 average in both the Arctic and Antarctic. The Arctic SIE maximum (14.42 million km2, 7th March), was the lowest winter maximum in the satellite record; however, the spring/summer melt was slower than in recent years and. thus, the summer end minimum (4.64 million km2, 13th September) was about 1.25 million km2 over the 2012 record low (WMO, 2018). In Arctic permafrost regions (Fig. 7), there has been a warming down to 20 m depth. Temperatures have increased in most regions by up to 2°C since 1980, leading to thawing and significant infrastructure damage. Generally, the thickness of the NH permafrost has decreased by 0.32 m since 1930 (IPCC, 2013).

Figure 6
Arctic and Antarctic sea ice extent (SIE) (P. Taalas, WMO, 2019)

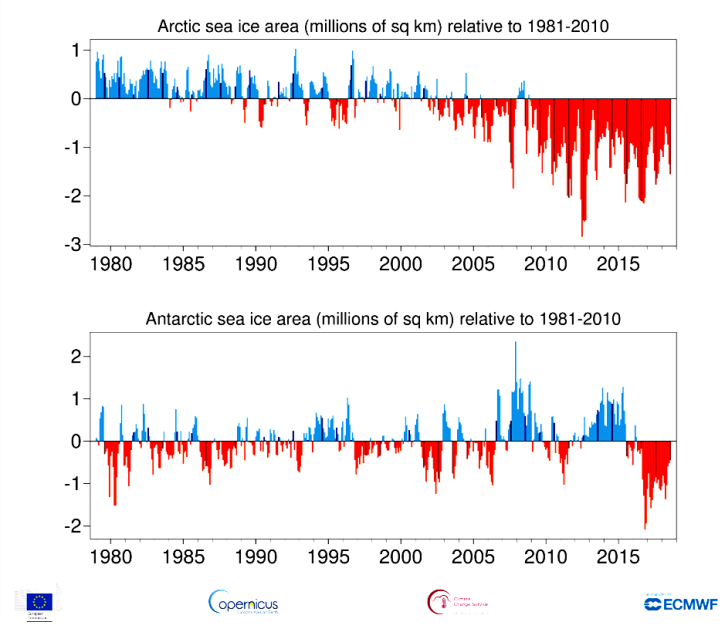

22. The (land) ice mass balances of Antarctica and Greenland are extremely important as they control (amongst others) the mean sea level rise (SLR). The Greenland surface mass balance-SMB did not show any significant trends in the 1960s, 1970s and 1980s, but it has started decreasing since the early 1990s (on average by 3 per cent per year). This has resulted in a statistically significant contribution to the mean sea level rise (SLR) rate (Hansen et al., 2016). The long-term trend for the Antarctic land ice appears flat. Recently, however, there have been worrying signs. It appears that the total mass loss increased from 40 ± 9 Gt year−1 in 1979–1990 and 50 ± 14 Gt year−1 in 1989–2000, to 166 ± 18 Gt year−1 in 1999–2009 and 252 ± 26 Gt year−1 in 2009–2017. The contribution to SLR from this land ice mass melt averaged 3.6 ± 0.5 mm per decade with a cumulative 14.0 ± 2.0 mm since 1979 (Rignot et al., 2019).

Figure 7

Map of the northern circumpolar permafrost zone, highlighting the extent of the yedoma type of permafrost soil (yellow and red) that accounts for significant portion of the permafrost carbon pool (Schuur et al., 2015 doi:10.1038/nature14338)

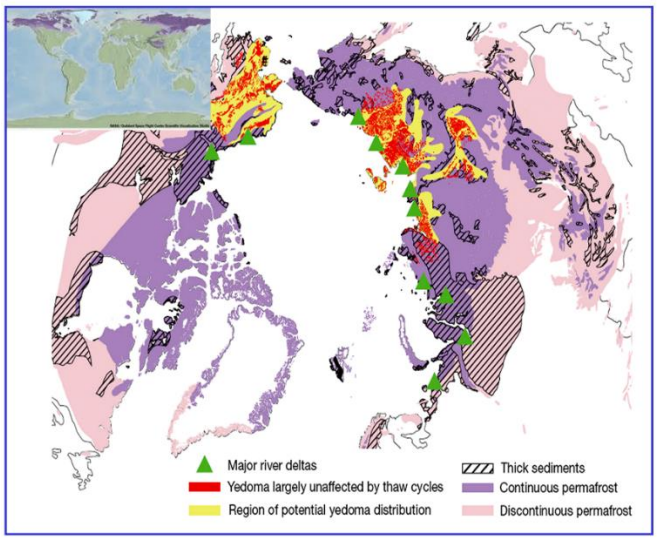

23. Velicogna et al. (2014) have estimated ice sheet loss rates in Greenland of 280 ± 58 Gt year−1, accelerating by 25.4 ± 1.2 Gt year−1. An ice mass loss rate of 74 ± 7 Gt year−1 was also observed in the nearby Canadian glaciers and ice caps with an acceleration of 10 ± 2 Gt year−1. Generally, mountain glaciers generally continued their melt. The vast majority of reference glaciers for which 2015 - 2016 data have been available show ice mass deficits less extreme than those of 2014 - 2015, but above the 2003–2015 average (WMO, 2017). In recent years, the western North American glaciers have lost 117 ± 42 gigatons (Gt) of mass, showing a fourfold increase in loss rate between 2000–2009 (2.9 ± 3.1 Gt yr-1) and 2009–2018 (12.3 ± 4.6 Gt yr-1); this may have been driven by the upper level zonal wind dynamics (Menounos et al., 2018).

2. Projections

24. Arctic snowfall has been projected to increase. Winter snow depth will increase over many areas, with the most substantial increase (15 to 30 per cent by 2050) taking place in Siberia. However, the snow has been projected to stand for 10 to 20 per cent less time each year over most of the Arctic, due to earlier spring melting (AMAP, 2012); thus, the spring snow cover extent (SCE) in 2100 is projected to decrease by about 25 per cent under the RCP8.5 (Fig. 8a). Mountain glacier mass has been also projected to decrease by 10 to 30 per cent by 2100 (AMAP, 2012). Recent research has estimated more substantial losses for the Hindu Kush - Himalaya glaciers (Wester et al., 2019).

25. Accelerating permafrost thawing is also projected due to rising global temperatures and changes in the snow cover. Current warming rates at the European permafrost surface are 0.04°C–0.07°C yr-1 (EEA, 2015a). Although there are challenges in the assessment of the permafrost dynamics (including those related to soil processes, climate scenarios and model physics), permafrost extent is expected to decrease by 37–81 per cent depending on the scenario by the end of the twenty-first century (medium confidence) (Fig. 8b). This could impose problems in the development/maintenance of Arctic infrastructure (ECE, 2013), which could constrain the development of transport networks to take advantage of the new Arctic Ocean routes made possible by the projected Arctic sea ice melt (Fig. 9).

Figure 8

Projected (a) snow cover extent (SCE) and (b) near-surface permafrost changes for 4 Representative Concentration Pathways-RCPs (CMIP5 model ensemble) (IPCC, 2013)

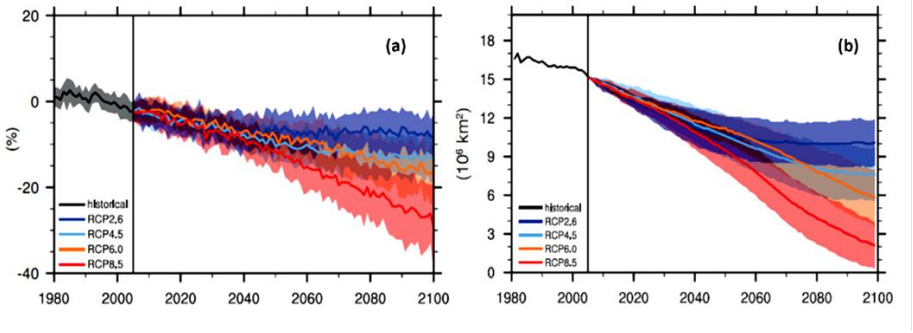

26. Based on the CMIP5 model ensemble, Arctic sea ice extent (SIE) is projected to decrease considerably, although there will be considerable inter-annual variability. In 2081–2100, reductions in SIE of 8–34 per cent (in February) and 43–94 per cent (in September) have been projected relative to the average SIE of 1986–2005, depending on the RCP scenario (IPCC, 2013).

Figure 9

New Arctic shipping routes (U.S. Climate Resilience Toolkit, 2015)

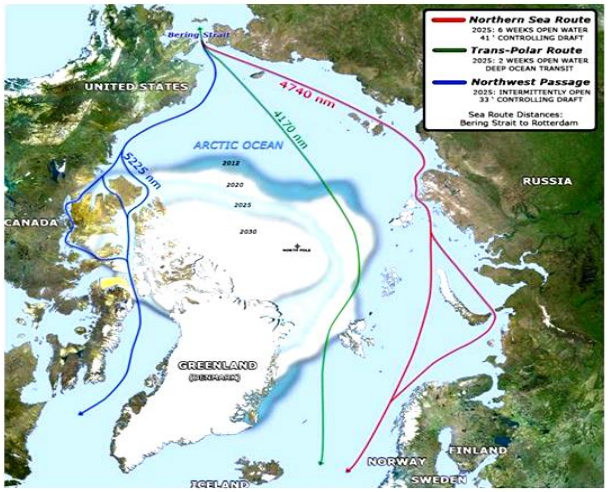

27. There may be new socio-economic opportunities for Arctic communities, as the shrinking sea ice promotes Arctic international shipping and facilitates access to substantial natural resources (e.g. the hydrocarbon deposits at Beaufort and Chukchi Seas). 3 major shipping routes are anticipated in the Arctic Ocean by 2025 (Fig. 9). Several seaports have been already developed in the Russian Federation to service commodity transport. In 2017, the cargo turnover in these seaports has increased by 1.5 times compared to 2016, reaching 73 million tons; by 2030, the turnover is expected to increase further to 140 million tons (Egorshev, 2018). There are, however, environmental risks and development challenges associated with the exploitation of the new Arctic routes. CV & C will affect existing and future infrastructure due e.g. to thawing permafrost and increased coastal wave activity, that will require specialized/innovative adaptation measures (Egorshev, 2018).

28. Global warming will impact the Greenland Ice Sheet (GIS), the surface mass balance (SMB) of which has recently shown an accelerating decreasing trend (Velicogna et al., 2014; Hansen et al., 2016). By comparison, the SMB of the Antarctic ice sheet has been projected to increase under most IPCC scenarios due to increasing snowfall (but see the recent observations of Rignot et al. (2019)). It should be noted that plausible decreases in the Antarctica SMB might increase the SLR by 2100 by more than 1 m (De Conto and Pollard, 2016).

D. Sea level and waves

1. Trends

29. The oceans, which may have absorbed more than 80 per cent of the excess energy associated with the increased emissions since the 1970s, show very significant increases in their heat content (Dieng et al., 2017; Cheng et al., 2019a) which have resulted in steric sea level increases, a major contributor to the SLR (Hanna et al., 2013). In recent decades, the SLR rate increased sharply above the relatively stable background rates of the previous 2000 years (Church et al., 2013).

Figure 10
(a) Estimated sea level change (mm) since 1900. Data through 1992 are the tide-gauge records with the change rate multiplied by 0.78, so as to yield a mean 1901–1990 change rate of 1.2 mm year−1 (Hansen et al., 2016)
(b) Global mean sea-level (seasonal cycle removed), January 1993–January 2018, from satellite altimetry. Data from AVISO (Source: Collecte-Localisation-Satellite (CLS) – Laboratoire d'Etudes en Géophysique et Océanographie Spatiales (LEGOS) (WMO, 2018)

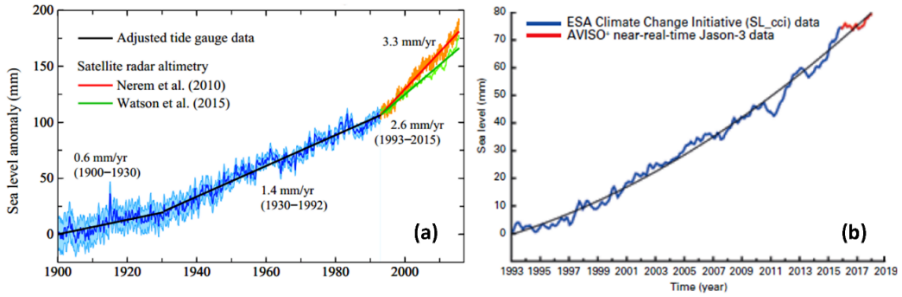

30. Since 1860, global sea level has increased by about 0.20 m; during this period, global SLR rates averaged 1.3–1.8 cm per decade (Church et al., 2013; Hay et al., 2015). The upward trend in sea level has varied over the decades. There were lower rates of increase during the early part of the twentieth century and most of the 1960s and 1970s, whereas sea level increased more rapidly during the 1930s and through the 1950s (Fig. 10). Since 1993, satellite and tide gauge observations indicate a global SLR of 3.3 ± 0.25 cm per decade (Church et al., 2013), with the acceleration being attributed mainly due to ice mass balance changes rather than steric effects (Dieng et al., 2017b; Rignot et al., 2019).

31. There is considerable regional (spatial) variability in the coastal sea level rise (Menendez and Woodworth, 2010). In Europe, sea levels have increased along most of its coast in the last 40 odd years, with the exception of the N. Baltic coast (EEA, 2012). Some regions experience greater SLR than others, as e.g. the tropical western Pacific. Sea level rise has been more consistent in the Atlantic and Indian Oceans, with most areas in both oceans showing rates similar to the global average (WMO, 2016).

2. Projections

32. Process-based predictions of the SLR are constrained by uncertainties on the response to global warming and the variability of: the GIS and AIS mass balance (Hansen et al., 2016; Rignot et al., 2019); the steric changes (Cheng et al., 2019a; 2019b); the contributions from mountain glaciers (Menounos et al., 2018); and the groundwater pumping for irrigation purposes and the storage of water in reservoirs (Wada et al., 2012).

Figure 11

(a) SLR projections for 2100. Key: 1, IPCC (2007a), 0.18 - 0.59 m; 2, Rahmstorf et al. (2007); 3, Horton et al. (2008); 4, Rohling et al. (2008); 5, Vellinga et al. (2008); 6, Pfeffer et al. (2008); 7, Kopp et al. (2009); 8, Vermeer and Rahmstorf (2009); 9, Grinsted et al. (2010); 10, Jevrejeva et al. (2010); 11, Jevrejeva et al. (2012); 12, Mori et al. (2013); 13, IPCC (2013); 14, Horton et al. (2014); and 15, Dutton et al. (2015). The variability reflects differences in assumptions/approaches
(b) Global SLR in the twenty-first century relative to 1986-2005 (IPCC, 2013)

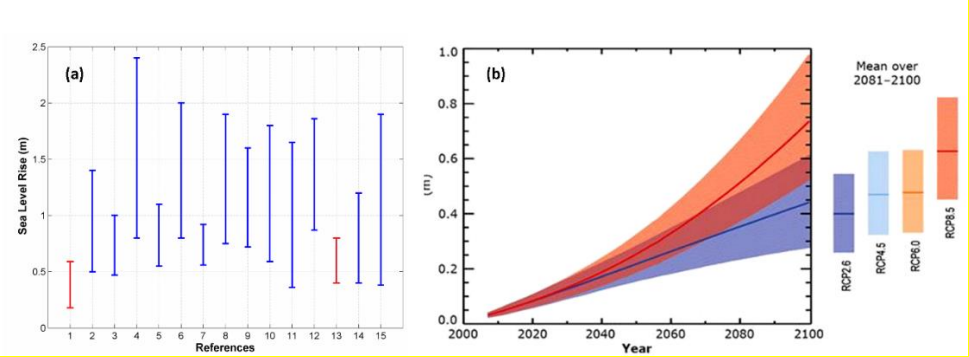

33. SLRs in 2081 – 2100 have been projected by IPCC (2013) as 0.26 – 0.54 m (RCP2.6) and 0.45 – 0.82 m (RCP8.5), compared to 1986 – 2005 (IPCC, 2013). It should be noted that the IPPC has consistently provided conservative estimates (Fig. 11). Due to the large spatial variability observed (and projected) in SLR, regional trends should be considered when assessing potential impacts along any particular coast. In addition to the global processes, regional factors can contribute to coastal sea level changes, such as changes in ocean circulation, differential rates in regional glacial melting, glacio-isostatic adjustment and the coastal sediment subsidence (King et al., 2015; Carson et al., 2016; Jevrejeva et al., 2016).

34. Sea level rise will continue beyond 2100 (Jevrejeva et al., 2012), due to the rising ocean heat content (Cheng et al., 2019a) that will induce increasing thermal (steric) expansion for (at least) several centuries, whereas dynamic ice loss in Antarctica and Greenland will also continue well into the future. Unchecked mean temperature rises may induce runaway sea level rises. Global warming of 2°C above the pre-industrial level[5] has been widely suggested as a threshold beyond which climate change risks become unacceptably high (but see IPCC (2018)). Without effective mitigation measures, this threshold is likely to be reached in about 2050 under the RCP8.5.

35. Probabilistic SLR projections with warming at and above the 2°C show that more than 90 per cent of the global coastline will experience rises exceeding the global estimate of 0.2 m, with rises up to 0.4 m expected along the Atlantic coast of North America (Fig. 12). By comparison, under a 5°C rise (close to the upper limit of the projected

[5] The limit goal of the 2015 Paris Agreement (unfccc.int/process#:a0659cbd-3b30-4c05-a4f9-268f16e5dd6b)

temperature rise in 2100, IPCC, 2013), SLR will reach 0.9 m (median), and 80 per cent of the coastline will exceed the global SLR at the 95th percentile upper limit of 1.8 m (Jevrejeva et al., 2016). Palaoclimatic, instrumental and modeling studies have shown that combinations of global and regional factors can cause relatively rapid SLR rates along particular coasts (e.g. Cronin, 2012).

Figure 12

Regional sea level projections for warming under the RCP8.5: (A and B) 2°C, (C and D) 4°C, and (E and F) 5°C relative to 1986–2005. A, C, and E show median (50 per cent) projections, and B, D, and F show upper limits (95 per cent) projections. Black contours show SLR (in m), whereas white contours correspond to zero SLR (Jevrejeva et al., 2016)

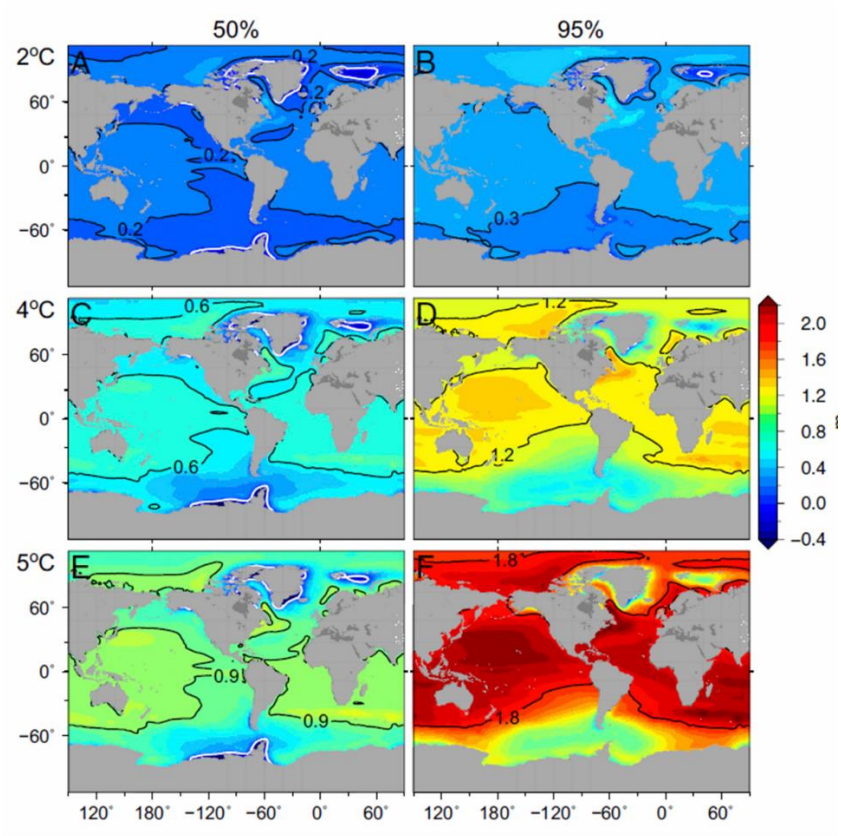

36. In Europe, both the current trends and future projections suggest substantial regional SLR variability (Fig. 13). For the Netherlands coast, Katsman et al. (2011) have estimated sea level rises of 0.40–1.05 m for a plausible high end emission scenario, whereas a SLR of up to 0.8 m has been projected for the Mediterranean region in 2100 (Hinkel et al., 2014; Jevrejeva et al., 2016). In addition to SLR, the impacts on coastal transport infrastructure/operations depend also on other factors/hazards, such the mean and extreme wave conditions and storm surges. Camus et al. (2017) have provided global multi-model projections of wave conditions (e.g. significant wave height[6]) under climate change

[6] Annual significant wave height (Hs) is the mean of the highest one third of the waves recorded at a site in each year.

(Fig. 14) to assist assessments on the impacts of CV & C on coastal transport infrastructure (Asariotis et al., 2017).

Figure 13

Left: Trends in absolute sea level in European Seas from satellite measurements (1992–2013) (EEA, 2014b). Right: Projected change (CMIP5 ensemble) in relative sea level in 2081 - 2100 compared to 1986 - 2005 for the moderate emission scenario RCP4.5. No projections are available for the Black Sea (EEA, 2014c).

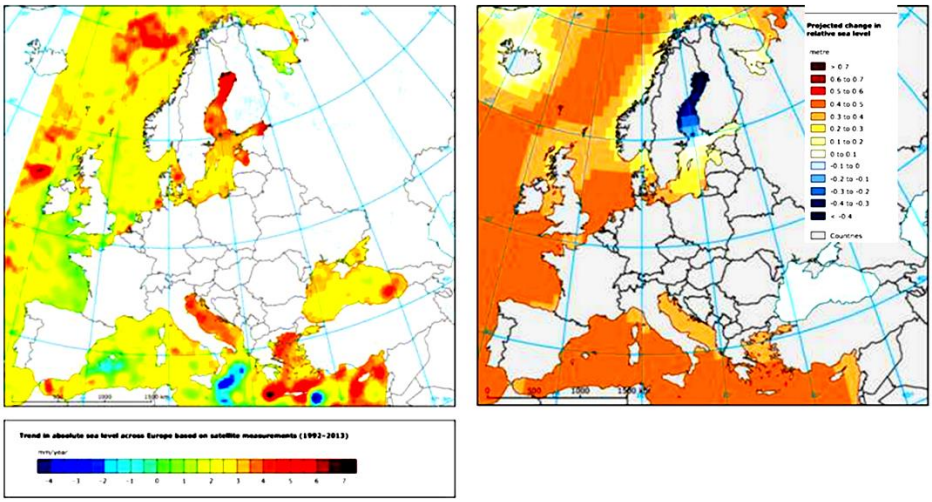

37. The annual mean Hs has been projected to increase in the Southern Ocean and the eastern Pacific and to decrease in the north Atlantic, the northwestern Pacific and the Indian Oceans, with the magnitude of the increases being about four times higher than those of the decreases. If these projections are considered together with the SLR, then seaports in some areas could be compromised by increased sensitivity of their (low) breakwaters (Camus et al., 2017).

Figure 14

(a) Multi-model annual mean significant wave height (m) for the time period 1979–2005

(b) Multi-model projected changes in annual mean significant wave height for 2070–2100 relative to 1979–2005 under RCP8.5. Stippling represents areas where the magnitude of the ensemble mean exceeds inter-model standard deviation (Camus et al., 2017)

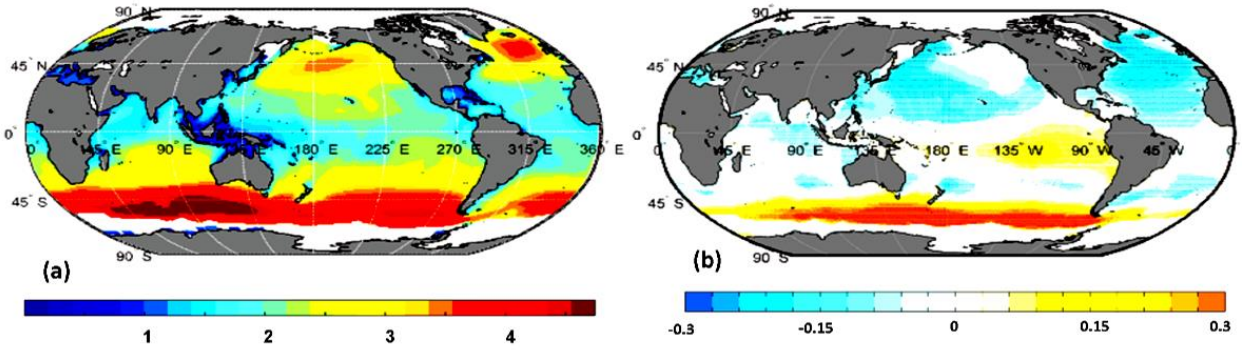

E. Extreme Climate Events

38. Climate change is often characterized in the public discourse by the increase in global mean temperature. However, for the transportation industry, as well as for the society, economy and the environment, regional conditions and changes in the climatic extremes can be the most relevant (Vogel et al., 2017). Changes in the mean climate can lead to changes in the frequency, intensity, spatial coverage, duration, and timing of weather and climate extremes, potentially resulting in unprecedented extremes. These extremes can, in turn, modify the distributions of the future mean climatic conditions (IPCC SREX, 2012). Extreme cover a large spectrum, such as sudden and transient temperature changes, rapid retreats of sea ice, bouts of abnormally high precipitation, intensive storms, storm surges, extended droughts, heat waves and wildfires and sudden water releases from melting glaciers and permafrost slumping; all these by themselves or in combination can have large and costly impacts on transport infrastructure and operations.

39. Extreme events, as well as changes in the patterns of particular climatic systems, e.g. the monsoons (King et al., 2015), can be the most impacting climatic phenomena at smaller spatio-temporal scales, since they can induce abrupt and more severe effects and natural disasters than changes in the mean climatic factors. Societies are rarely prepared to efficiently face extreme weather events, having become dependent on predictable, long-term climatic patterns (MetOffice, 2014). Most natural disasters are due to extreme hydro-meteorological events, such as floods and storms which account for about 44 and 28 per cent, respectively, of all natural disasters recorded in 1998–2017 (Taalas, 2019). In the United States of America (USA) these are responsible for 90 per cent of all US President-declared disasters as a substantial slice of the economy (about US$3 trillion) is sensitive to weather/climate (NOAA, 2017c).

40. In recent years, there have been many extreme events that have affected the Economic Commission for Europe (ECE) region and its transport infrastructure and operations, with some of those causing very severe damages/losses: the Hurricane Sandy in the Caribbean and the US (2012), droughts in the southern and central US (2012 and 2013), floods in central Europe (May–June 2013) and the 2017 hurricane season (Section II.E.3). Fortunately, human loss did not follow the steep upward trend in economic losses (NOAA, 2017c). However, Typhoon Haiyan (Yolanda) in the Philippines and flash floods in N. India resulted in 13,600 deaths (2013), whereas more than 3,700 people lost their lives from heat waves in India and Pakistan (May–June 2015)[7]. In terms of economic losses, the 1980–2016 average has been 5.5 disaster events per year with costs in excess of 1 US$ billion (CPI-adjusted), whereas the annual average for 2012–2016 has been 10.6 such events (NOAA, 2017c).

41. Many climate extremes show changes consistent with global warming, including a widespread reduction in the number of frost days in mid-latitude regions and discernible evidence that warm extremes have become warmer and cold extremes less cold in many regions (IPCC SREX, 2012). There is also a general change in the frequency of high impact temperature and precipitation extremes over land, irrespective of the type of dataset and processing method used (MetOffice, 2014). A slight decrease in the annual number (globally) of mild days (i.e. days with maximum temperature between 18°C – 30°C and precipitation < 1 mm) is projected for the near future (4 days/year for the 2016–2035 and 10 days/year for the 2081–2100) (Van der Wiel et al., 2017).

[7] The most lethal climatic extreme in recent years has been the 2010–2011 drought in Somalia that caused the 2010–2012 Somalia famine, considered responsible for more than 258,000 deaths (WMO, 2016).

42. It should be mentioned that, in many cases, the hazard related to the extremes of a particular climatic factor can be exacerbated by the simultaneous presence of another hazard(s), such as combined marine and riverine flooding (Forzieri et al., 2016). A combined hazard which might have very significant implications for the health/safety of personnel and passengers in most modes of transport is the combination of extreme heat with high relative humidity -the Heat Index (Monioudi et al., 2018). Recent research (Mora et al., 2017) indicates the presence of a 'deadly threshold' for the surface air temperature/relative humidity over which the human thermoregulatory capacity is exceeded (Fig. 15). Around 30 per cent of the world's population is currently exposed to climatic conditions exceeding this deadly threshold for at least 20 days a year and projections suggest that there will be a very significant deterioration in the course of the century (Section II.E.1).

Figure 15

Lethal heat events (1980-2014). a, locations with documented relationships between heat and mortality (red squares) and where specific heat events have been studied (blue squares). b, mean daily surface air temperature and relative humidity during lethal events (black crosses) and during periods of equal duration from the same locations but from randomly selected dates (I.e. non-lethal events; red to yellow). Blue line is the threshold that best separates lethal and non-lethal events; red line is the 95per cent probability deadly threshold (Mora et al., 2017).

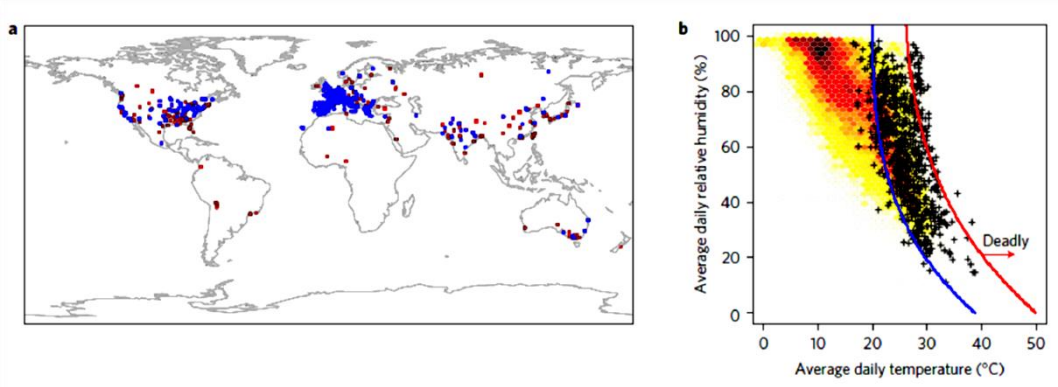

1. Temperature extremes - Heat waves: Trends and Projections

43. There is evidence suggesting increases in the frequency and intensity of heat waves (e.g. Beniston and Diaz, 2004; IPCC, 2013); there has been a 3-fold increase since 1920s in the ratio of the observed monthly heat extremes to that expected in a non-changing climate (Coumou and Rahmstorf, 2012). In recent decades, most of North America appears to have been experiencing more unusually hot days and nights, fewer unusually cold days and nights and fewer frost days (ECE, 2013). With mean temperatures continuing to rise, models project that increases in the frequency/magnitude of hot days and nights and decreases in the cold days and nights are virtually certain (IPCC, 2013). Heat waves are often associated with severe droughts (as e.g. during the European 2003 heat wave). Droughts have also become more severe in some regions, a trend that projected to hold (and, possibly, increase) in the twenty-first century (IPCC, 2013).

44. Heat waves have been recorded in Europe in 2012, 2013 and 2014. In Austria, it was the first time that temperatures reached 40 °C or above. A prolonged heat wave affected many parts of eastern Asia in July - August 2013 (WMO, 2014). Intense heat waves (temperatures at, or above 45 °C) were recorded in May - June 2015 in India and Pakistan with many human casualties (WMO, 2016). In western and central Europe, the worst heat wave since 2003 was recorded in early July 2015, with Spain, France and Switzerland

breaking all time temperature records; a few weeks later, temperatures of 40.3 °C were also recorded in Germany. In 2017 there were also numerous heat waves which affected Turkey and Cyprus (late June – early July), Spain and Morocco (mid-July), and Italy and the Balkans (early August). All-time records were set in: Antalya, Turkey (45.4°C, 1st July), Cordoba (46.9°C, 13th July) and Granada (45.7°C, 12th July) in Spain; and Pescara (41.0°C, 4th August), Campobasso (38.4°C, 5th August) and Trieste (38.0°C, 5th August) in Italy. Death Valley (USA) recorded the highest ever mean July temperature (41.9°C) in the country. Record-high temperatures occurred also in California in September (41.1°C in San Francisco) (WMO, 2018).

Figure 16

Median of the projected number of heat waves (from a model ensemble) in the near (2020–2052) and long (2068–2100) term under the RCP4.5 and RCP 8.5 scenario (EEA, 2015b).

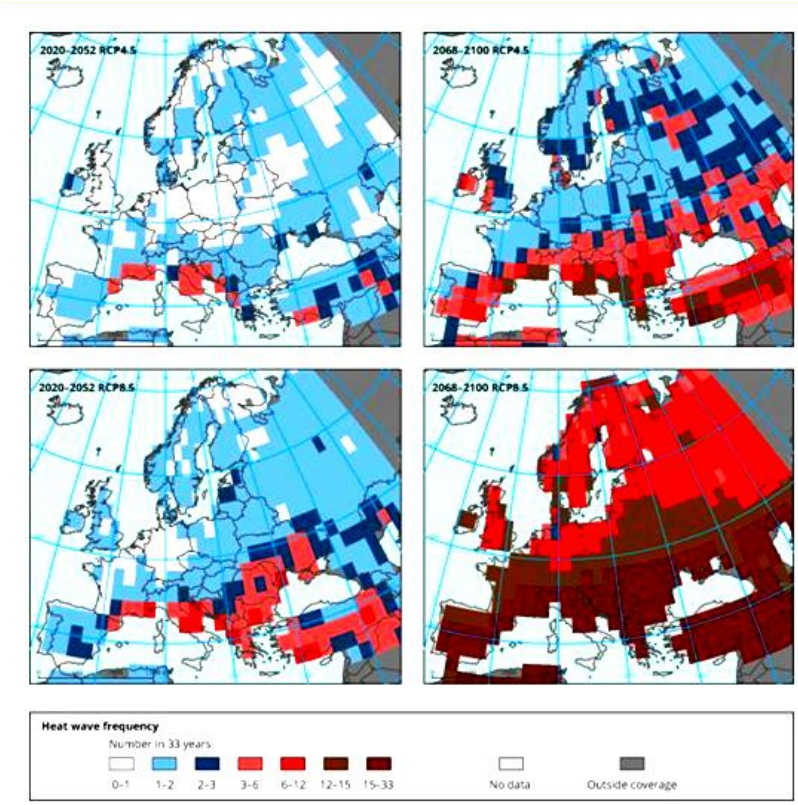

45. Increases in hot extremes and decreases in cold winter extremes are expected by the end of the twenty-first century, with the frequency, duration and magnitude of the events being affected by anthropogenic forcing (IPCC, 2013). Greater changes in hot (seasonal) extremes are expected to take place in the subtropics and the mid-latitude regions, whereas the frequency of cold events will decrease in all regions. Generally, very hot summers are projected to occur much more frequently in the future under all Climate Change scenario (Coumou and Robinson, 2013).

46. It is also likely that the frequency of heat waves (prolonged periods of excessive heat) in e.g. Europe will increase, mainly due to the increasing seasonal summer temperatures. For most land regions it is likely that the frequency of a current 20-year hot event will be doubled (in many regions it might even occur every 1–2 years), while the occurrence of a current 20-year cold event will be reduced under the RCP8.5 scenario

(IPCC, 2013). Large increases in heat waves are projected for large parts of the ECE region, particularly under RCP8.5 (Fig. 16).

47. Heat waves as severe as that of 2003 are expected to occur about once a century in the current climate; in early 2000s, such events were expected to take place approximately once every several thousand years. An attribution study has suggested that anthropogenic influence has at least doubled their probability of occurrence (MetOffice, 2014). Other studies suggest that the probability of occurrence of an extreme heat wave like that occurred in the Russian Federation in 2010 may increase by 5–10 times until 2050 (Dole et al., 2011).

Figure 17

Deadly climatic conditions in 2100 under different emission scenarios. Conditions refer to the number of days per year exceeding the threshold of temperature and humidity beyond which climatic conditions become deadly (see Fig. 10), averaged between 1995 and 2005 (historical experiment), and between 2090 and 2100 under RCP 4.5 and RCP 8.5. Results are based on multi-model medians. Grey areas indicate locations with high uncertainty (multi-model standard deviation larger than the projected mean) (Mora et al., 2017).

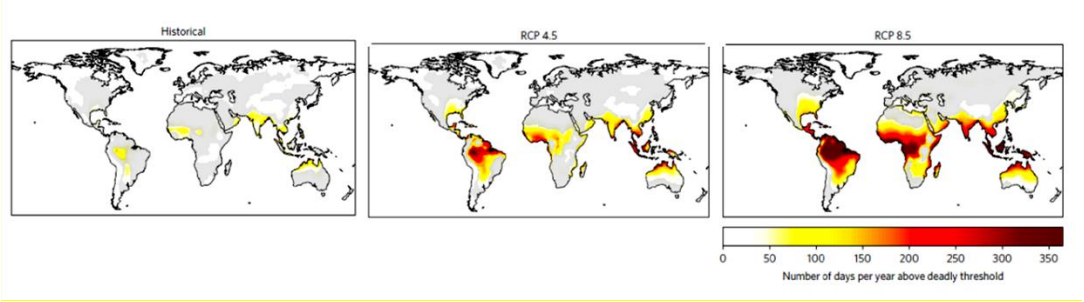

48. As mentioned earlier, the combination of extreme heat with high relative humidity- the Heat Index- may have very significant implications for the health/safety of personnel and passengers in most modes of transport. Projections (Mora et al., 2017) indicate substantial exceedance of the deadly threshold (Fig. 15) by the end of the century, which will be particularly severe under the now 'business as usual' scenario (RCP8.5), with direct impacts on southwestern USA and the Mediterranean ECE region (Fig. 17).

2. Heavy rainfalls and droughts: Trends and Projections

49. One of the clear trends appears to be the increasing frequency and intensity of heavy precipitation events (downpours). The increase has caused most of the observed increases in overall precipitation during the last 50 years and projections from climate models suggest that these trends will continue in this century. Slope failures/landslides have also increased at mountainous areas, as they are linked to heavy downpours (Karl et al., 2009).

50. River flooding from heavy precipitation is a most serious and widespread hazard (King et al., 2015). Between 1980 and 2014 river floods accounted for 41 per cent of all loss events, 27 per cent of fatalities and 32 per cent of economic losses (Munich Re, 2015). Recently, the flooding caused by the extremely heavy downpours during the Hurricanes Harvey (2017) and Florence (2018) was particularly destructive for the southern and eastern USA. Riverine floods are caused by both physical and socio-economic factors. The former depend on the hydrological cycle, which is influenced by changes in temperature, precipitation and glacier/snow melts, whereas the latter by land use changes, river management schemes, and flood plain development (EEA, 2010).

Figure 18

Current flood hazard (95 per cent probability) in the Eurasian region of the ECE for the 100-year flood from a global GIS model based on river discharge time-series. DEM resolution 90 m. Areas over 60 0N are not fully covered (From UNEP-GRID and UNISDR, 2008). (ECE, 2013).

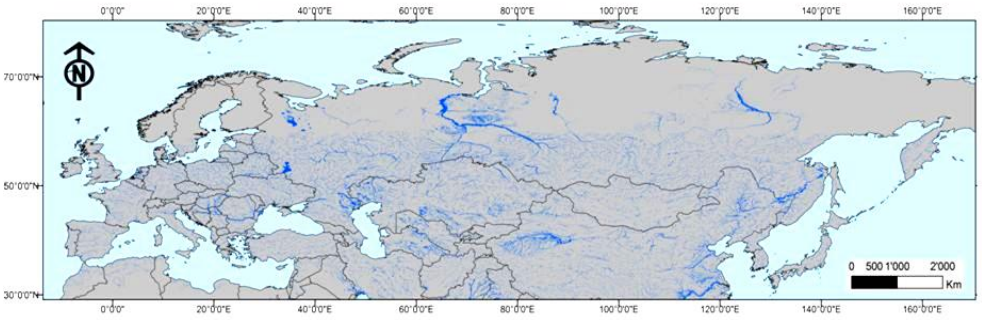

51. In the ECE region, floods are an ever present hazard. The current trends in the Eurasian countries show a significant flood hazard (for the 1 in a 100-year event), particularly for the central and eastern Europe, central Asia and along the large S-N trending Siberian drainage basins (Fig. 18). In Europe, annual water discharges have generally increased in the north and decreased in the south (e.g. EEA, 2012), trends that are projected to hold in the future (Alfieri et al., 2018) being driven by the projected precipitation changes (EEA, 2015c).

52. North America experienced severe droughts in 2012 and 2013. In July 2012, 64.5 per cent of the US territory was classified as experiencing droughts, the largest areal extent since the 1930s. Total rainfall in 2011–2016 was 30 per cent below normal, resulting in economic losses of about US$60 billion. Long-term droughts also occurred in Australia and southern Africa, whereas the Indian monsoon rainfall (June–September) was about 10 per cent below normal in both 2014 and 2015 (WMO, 2016). In 2017, many Mediterranean areas also experienced severe droughts, as did parts of central Europe. Italy had its driest January – August period on record (rainfall 26 per cent below the 1961–1990 average), Spain its driest autumn on record and Portugal its third driest year on record. Eastern Mediterranean was also badly affected. There were also severe droughts in North America. The 2016–2017 winter brought heavy rainfall to California; however, dry conditions resumed in the second half of the year (WMO, 2017; 2018). Regarding wildfires, 2017 was an active year, particularly for Portugal and NW Spain, Croatia, France and Italy and the western North America. Total economic losses for the 2017 California wildfires were assessed as US$18 billion, with the total area burnt in the contiguous USA being 53 per cent above the 2007−2016 average, just short of the 2015 record (WMO, 2018). 2018 also showed increased wildfire activity as e.g. in California and Greece.

53. Extremes linked to the water cycle (heavy rainfalls, floods and droughts) are already causing substantial damages. As temperature rises, average precipitation will exhibit substantial spatial variation. It is likely that precipitation will increase in the high and mid latitude lands and decrease in subtropical arid and semi-arid regions by the end of the century under the RCP8.5 scenario. Extreme precipitation events will be more intense over most of the mid-latitude and wet tropical regions (IPCC, 2013). For central and NE Europe, projections show large increases (25 per cent) in heavy precipitation by the end of the century (Fig. 19). High resolution climate models indicate that extreme seasonal rainfalls could also intensify with climate change; in the United Kingdom (UK), for instance, although summers will become drier overall, the occurrence of heavy summer downpours (more than 30 mm in an hour) could increase almost 5 times (MetOffice, 2014).

Figure 19

Projected changes in heavy precipitation (in per cent) in winter and summer from 1971 - 2000 to 2071 – 2100 for the RCP8.5 scenario based on the ensemble mean of regional climate models (RCMs) nested in general circulation models (GCMs) (EEA, 2015c).

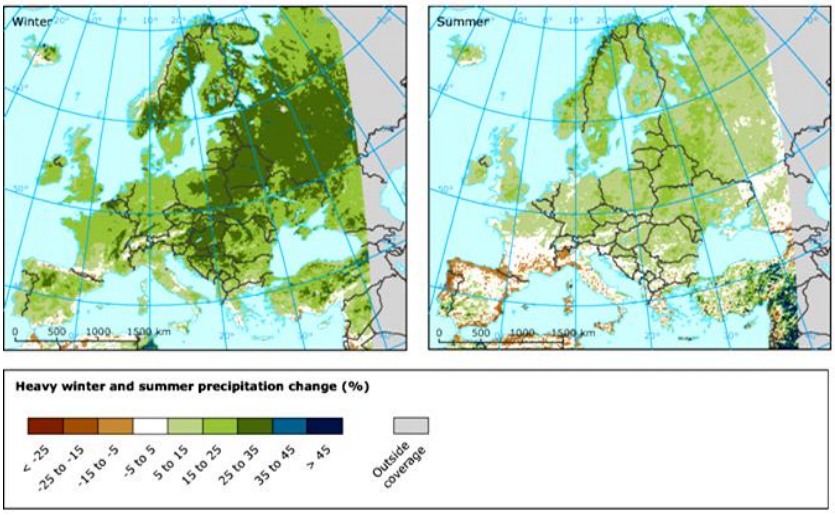

54. River flooding poses a most significant threat to transport infrastructure (ECE, 2013), as well as to global population. Increases in extreme runoffs have been well documented (Feyen et al., 2010), but the increasing damage/losses could be also attributed due to the increasing human and infrastructure exposure in the flood plains (IPCC, 2013). Large potential increases in river floods for the most European areas are projected by the end of the century (Fig. 20). Recent research (Alfieri et al., 2015) has indicated that global warming will be also linked to substantial increases in riverine flood risk over most central and western Europe (no model agreement for eastern Europe). The expected flood damages under a 1.5°C temperature rise since the pre-industrial times (IPCC, 2018) were assessed by a model super-ensemble as € 15 billion/year, more than double the average costs of 1976–2005. Damages from riverine floods are expected to be generally higher in the north than in the south (Alfieri et al., 2015; 2018)

Figure 20

Relative change in the 100-year river floods for a) 2020s, b) 2050s and c) 2080s compared to 1961-1990 for SRES A1B scenario (roughly equivalent to RCP6.0) (EEA, 2012)

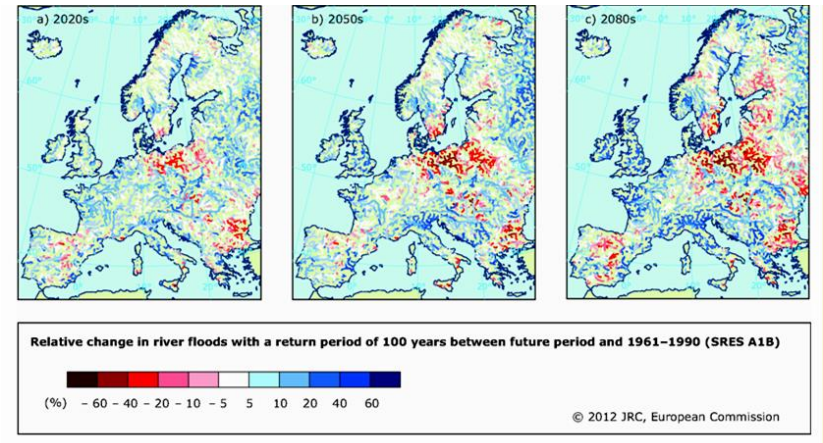

55. Climate variability and change (CV & C) is projected to raise by > 50per cent the numbers of people affected by the current 30-year flood. By the 2050s, there is at least a 50 per cent chance that climate change alone could lead to a 50 per cent increase in flooded people across sub-Saharan Africa, and a 30–70 per cent chance that such an increase would also take place in Asia. By 2100, risks will be higher. Population change alone will increase the numbers of people affected by flooding. The global total will increase very substantially (by about 5–6 times) over the century under RCP8.5. Concerning the ECE region, flood impacts in 2050 (see above) are projected to be generally milder than in the other regions; nevertheless, the conditions in some ECE regions (e.g. the USA) are projected to deteriorate by 2100 ((King et al., 2015).

3. Storms and high winds: Trends and projections

56. There is evidence indicating that storms and waves may respond to a warming climate by becoming more extreme (e.g. Emanuel, 2005; Ruggiero et al., 2010; WMO, 2014). It appears that although the annual incidence of tropical storms has not changed with time (WMO, 2018), their ferocity (and impacts) have been amplified, probably by the increasing ocean heat content and surface temperatures (Trenberth et al., 2018). The implications for e.g. the coastal communities and transport infrastructure could be severe due to, amongst others, increases in the extreme sea levels (ESLs) and waves (Vousdoukas et al., 2018; Monioudi et al., 2018). It should be noted that storms can induce combined hazards (e.g. both riverine and coastal flooding and high wind damages).

57. 2017 was the year with the highest documented economic losses associated with extreme hydro-meteorological events (WMO, 2018), due mainly to a very active North Atlantic hurricane season, major monsoon floods in the Indian subcontinent, and severe droughts in east Africa. In 2018, there were also major tropical storms, some of which developed very rapidly. These included Hurricanes Florence and Michael in the Atlantic and the strong typhoons Jebi and Manghut (the most intense 2018 storm with winds of 287 km h−1) and Trami in the Pacific. Some of these storms caused major flooding, especially Florence (Carolinas, SE USA) and Olivia and Lane (Hawaii). Lane induced the second-highest rainfall (after Harvey) from a tropical cyclone in the USA since 1950 (Cheng et al., 2019b).

58. Although the overall number of tropical cyclones (84) in 2017 was close to the long-term average, some (mainly in North Atlantic) were particularly ferocious. Three exceptionally destructive hurricanes developed in the North Atlantic in late August - September devastating the coastal areas of the southern USA as well as several Caribbean islands including overseas territories of ECE Member States (e.g. Puerto Rico, the British Virgin Islands, and the Saint Martin and Sint Maarten).

Figure 21

Transport infrastructure damages from the 2017 hurricanes. (a) Harvey: highway flooding in downtown Houston (USA) (www.pbs.org/newshour/science/hurricane-harvey-became-extreme). (b) Harvey: Houston highways (www.vox.com/science-and-health/2017/8/28/16211392/100-500-year-flood-meaning). (c) Maria: Bridge at Puerto Rico) (https://coastalresiliencecenter.unc.edu/2018/10/lessons-learned-from-hurricanes-irma-and-maria/). (d) Destruction of the Sintt Maarten Princess Juliana international airport by Hurricane Irma (September 2017) (sxmgovernment.com/2017/09/07/new-photos-hurricane-irmas-destruction-of-st-maartens-princess-juliana-international-airport/)

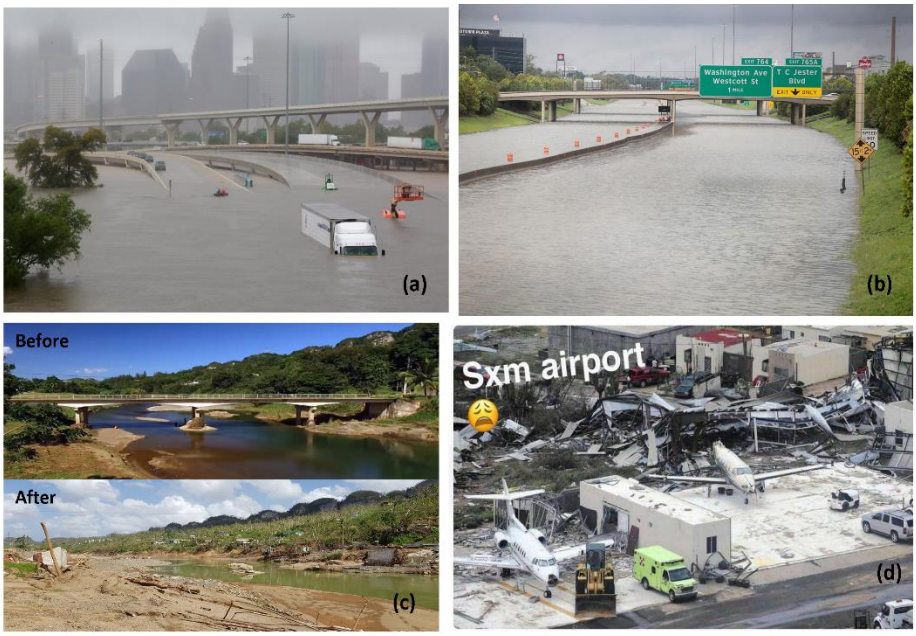

59. Harvey made landfall in south Texas as a category 4 hurricane and remained almost stationary over Houston for several days, producing prolonged downpours and severe flooding (Fig. 21); 1539 mm of rain fell between 25/08/2017 and 01/09/2017 (annual exceedance probability less than 1 in 1000). Trenberth et al. (2018) suggested that this event had been made 3 times more likely by anthropogenic climate change. Hurricanes Irma (category 5, early September) and Maria (category 5, mid September) followed. Irma's landfall led to extreme damages across many Caribbean islands (Barbuda, Saint Martin/Sint Maarten, Anguilla, St Kitts and Nevis, the Turks and Caicos, Virgin Islands, the southern Bahamas and Cuba). Maria made initial landfall on Dominica (total damages/losses estimated as US$ 1.3 billion – 224 per cent of GDP), before it continued towards Puerto Rico where it induced severe and widespread human losses and damages. These hurricanes were responsible for more than 320 deaths and assessed by the National Center for Environmental Information (NCEI) as ranking in the top five for hurricane-related economic losses in the USA (with Katrina (2005) and Sandy (2012)), with estimated losses of US$ 95 billion (Harvey), US$ 70 billion (Maria) and US$ 81 billion (Irma) (Taalas, 2019).

Figure 22

Top: Current incidence (244) of Category 4 and 5 storms (244). Bottom: Incidence (313) of Category 4 and 5 storms under 2°C global warming relative to the pre-industrial times (in 2100, under RCP4.5) (Taalas, 2019).

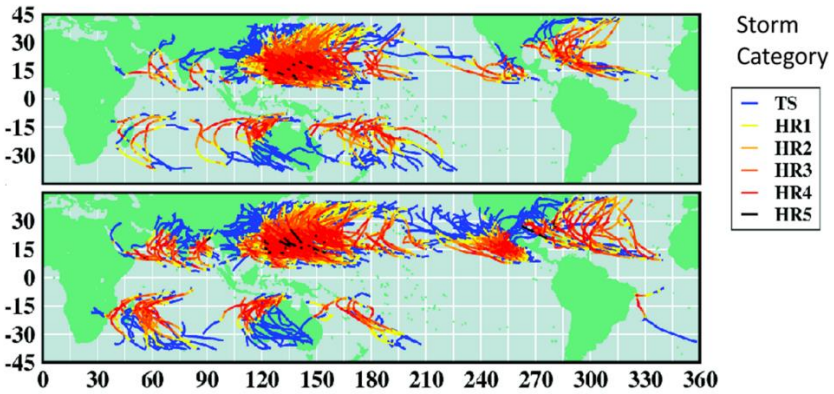

60. In 2012–2015, high wind and tornado activity in the USA was below the 1991–2010 average, but Europe encountered several extra-tropical cyclone-associated windstorms. In 2013, Denmark experienced extreme winds (53.5 m/s) that caused excessive damage. The highest storm surge levels since 1953 were recorded in Netherlands and the UK. In the UK, the 2013–2014 winter was the wettest on record and there were also severe wind damages and coastal erosion (WMO, 2016). In 2016, tornado activity in the USA was below its long-term average (985 tornadoes, 10 per cent less than the post-1990 average). There were, however, hailstorms resulting in damages in excess of US$5 billion in Texas (WMO, 2017; NSIDC, 2017). In 2017, central and eastern Europe also suffered severe thunderstorms. Winds, exceeding 100 km/h resulted in widespread damages (and at least 11 deaths) in Moscow (29th May 2017). Noteworthy windstorms also occurred in Innsbruck, Austria (165 km/h wind gusts, 30th July) and in southern Finland (12th August). 2017 showed an above-average tornado season in the USA (1406 tornadoes, 12 per cent above the 1991–2010 average). A severe windstorm (Zeus) affected France in early March (193 km/h gusts in Brittany), whereas strong windstorms also occurred in Austria and the Czech Republic in late October, with gusts exceeding 170 km/h (WMO, 2018).

61. Storms and windstorms are difficult to predict. However, as the severe tropical and extra-tropical storms (which are usually associated with extreme winds, rainfall and coastal flooding) are fed by the increasing upper ocean heat content and temperatures, it is expected that these will deteriorate in the future. It has been suggested that a modest temperature rise by 1°C in the upper ocean might result in storm wind speed increases of up to 5 m/s as well as increased incidence of the most destructive (Category 5) cyclones (Steffen, 2009); this can have severe effects on the coastal (and inland) transport infrastructure (e.g. Becker et al., 2013). Recent research also project increases in the incidence of the most intensive tropical storms by the end of the century, even under a moderate warming scenario (Fig. 22).

4. Extreme sea levels and waves: Trends and projections

62. Coastal transport infrastructure can be impacted by coastal erosion and flooding which are driven by the extreme waves and sea levels (e.g. Ranasinghe, 2016; Rueda et al., 2017). Extreme sea levels (ESLs) are considered as the sum of the mean sea level (MSL), the astronomical tide (η_{tide}) and the episodic coastal water level rise (η_{CE}) due to storm surges and wave set ups. Therefore climate-driven changes in any of the above components will affect also the ESLs.

63. Mean sea level rise (SLR) amplifies ESLs (Marcos et al., 2011), as do increases in the storm surges. Documented changes in the intensity and frequency and/or the patterns of extreme waves (Ruggiero, 2013; Bertin et al., 2013; Pérez et al., 2014; Mentaschi et al., 2017) also do and will affect ESLs, as higher waves induce higher coastal wave set ups. Extreme sea levels and waves constitute a most severe threat to the coastal areas and related transport infrastructure and operations, with many coastal areas currently experiencing erosion and/or inundation from such events (Losada et al., 2013). These hazards are expected (with high confidence) to increase in the future due to the accelerating SLR, all other contributing factors being equal (Hallegatte et al. 2013; Vousdoukas et al., 2017).

64. ESLs are characterised by considerable regional variability, with large tracts of the northern ECE coast (e.g. western and eastern Canada, the North Sea and eastern Russia) showing very high values compared to the Mediterranean and Black Sea coasts (Fig. 24a). Extreme sea levels can pose a particular threat to highly developed, low-lying coasts such as the river deltas which are considered hotspots of coastal erosion/vulnerability due to their commonly high relative SLRs (ECE, 2013).

65. Global projections show that ESLs will increase during the twenty-first century in all areas, although there will be also regional variability (Fig. 23b and c). With regard to the storm surge component of the ESL, projections for Europe show larger storm surge levels for the Atlantic and Baltic coasts (and ports) under all scenarios tested (Vousdoukas et al., 2016a; Vousdoukas et al., 2017). North Sea, an area subject already to some of the highest storm surge levels in Europe, is projected to show increases, particularly along its eastern coast. Storm surges are projected also to increase along the Atlantic coast of the UK and Ireland, due mostly to a consistent increase in the winter extremes. By comparison, studies in the Mediterranean indicate small or no future changes, with a decrease in the frequency/intensity of extreme events being likely (Conte and Lionello, 2014; Androulidakis et al. 2015) or being mostly in the ± 5 per cent band (Vousdoukas et al., 2016a). This is in agreement with historical trends (Menéndez and Woodworth 2010). North Adriatic, a coast which has been more thoroughly studied due to its highly exposed Venice area, ihas been projected not to show any statistically significant changes in the storm surge levels (Mel et al. 2013, but see also Lionello et al. (2012).

Figure 23

Present global extreme sea levels (ESLs) and changes in view of climate change. Maps show the median present-day 100-year ESL (a) and the projected changes in ESLs100 expressed by the median under RCP4.5 (b) and RCP8.5 (c) by 2100 (Vousdoukas et al., 2018).

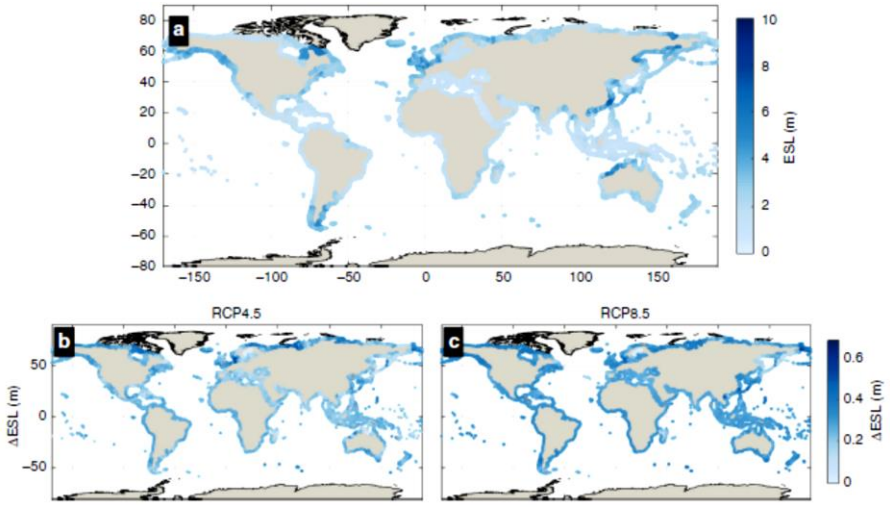

66. Averaged over Europe's coastlines, the present 100-year ESL (ESL100) is projected to occur approximately every 11 years by 2050, and every 3 and 1 years by 2100 under RCP4.5 and RCP8.5, respectively (Fig. 24). Hence, 5 million Europeans (and their transport infrastructure) currently at risk once every 100 years, may be flooded at an almost annual basis by the end of the century (Vousdoukas et al., 2016b; 2017). Some regions are projected to experience an even higher increase in the frequency of occurrence of extreme events, most notably along the Mediterranean and the Black Sea, where the today's ESL100 is projected to occur more often.

67. It should be noted that more than 200 million people worldwide live along coastlines with an elevation of less than 5 m above sea level; this figure is estimated to increase to 400–500 million by the end of the twenty-first century. Growing exposure (population and assets), rising sea levels due to CV & C, and in some regions, significant coastal subsidence due to human coastal water drainage/groundwater withdrawals will increase the flood risk to varying degrees. For instance, a 1 m rise in relative sea level may increase the frequency of current 100-year coastal flood events by about 40 times in Shanghai, about 200 times in New York, and about 1000 times in Kolkata (WMO, 2014).

Figure 24

Return period of the present day 100-year ESLs along the European coastline under RCP4.5 and RCP8.5 in 2050 (a) and 2100 (b). Colored boxes express the ensemble mean value and colored patches the inter-model variability (best-worst case (Vousdoukas et al., 2017).

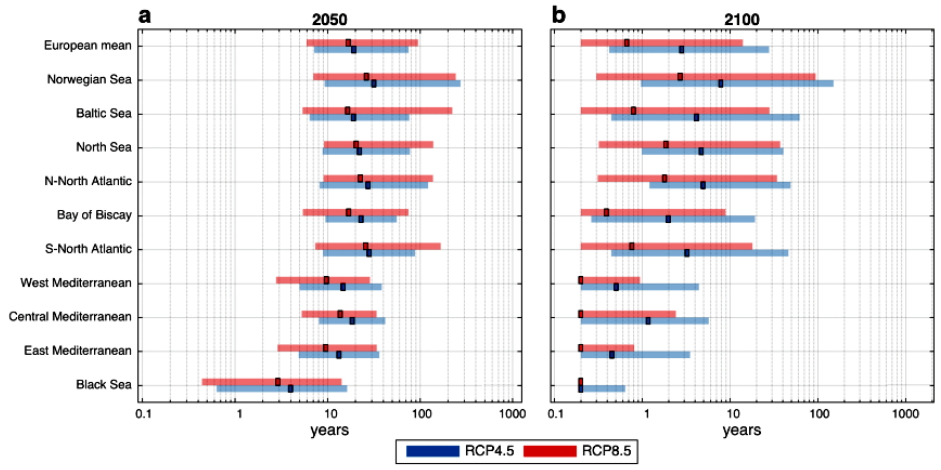

68. For the next 50 years or so, Hallegatte et al. (2013) have suggested for the 136 largest coastal cities that: (i) damages could rise from US$ 6 billion/year to US$52 billion/year due to increase in population and assets; (ii) annual losses could approach US$ 1 trillion or more per year if flood defenses are not upgraded; (iii) even if defenses would be upgraded, losses could increase as coastal floods could become more intense due to the SLR. This raises the question of whether there are potential thresholds which, if passed, could reverse the current and projected trends of coastal population and asset growth (King et al., 2015).

69. In terms the extreme waves, recent modeling results under the (RCP8.5) suggest an increase of up to 30 per cent in the 100-year return level of wave energy fluxes (WEF) for most coastal areas of the southern temperate zone, with the exception of Eastern Australia, the southern Atlantic, and the sub-equatorial-tropical E. Pacific (Mentaschi et al., 2017). By comparison, large coastal areas in the Northern Hemisphere are projected to have a negative trend, with the exception of the NE Pacific and the Baltic Sea which will show positive trends (increases of up to 30 per cent).

F. Forcing Mechanism

70. A major cause of the observed increases in the heat content of the planet is considered to be the rising concentrations of atmospheric Greenhouse Gases (GHGs) that enhance the "greenhouse effect", a well-documented and understood physical process of the Earth System since the ninteenth century (e.g. Canadell et al., 2007). GHGs absorb heat reflected back from the Earth's surface and, thus, store more heat in the ocean, land and atmosphere (IPCC, 2013). Without the greenhouse effect, the average temperature on Earth would be about -19ºC, i.e. about 34ºC colder than it is at present. All planets with heat absorbing gases in their atmosphere, experience a greenhouse effect. For example, the extreme hot temperatures of Venus are due to the high concentration of GHGs in its atmosphere.

71. Water vapor, an abundant GHG, makes a major contribution. The ability of the atmosphere to retain water vapor increases with global warming; thus, water vapor not only follows, but exacerbates changes in global temperature induced by the increasing concentrations of the other GHGs (e.g. Richardson et al., 2009; Shakun et al., 2012). The atmospheric concentrations of CO2, CH4 and the other GHGs have increased very substantially over recent decades (Fig. 25), probably as a result of human activities (IPCC, 2013).

Figure 25

Top row: Globally averaged mole fraction (measure of concentration) from 1984 to 2016, of CO2 in parts per million (left), CH4 in parts per billion (middle) and N2O in parts per billion (right). Bottom row: The growth rates representing increases in successive annual means of mole fractions for CO2 (left), CH4 (middle) and N2O (right) (WMO, 2018).

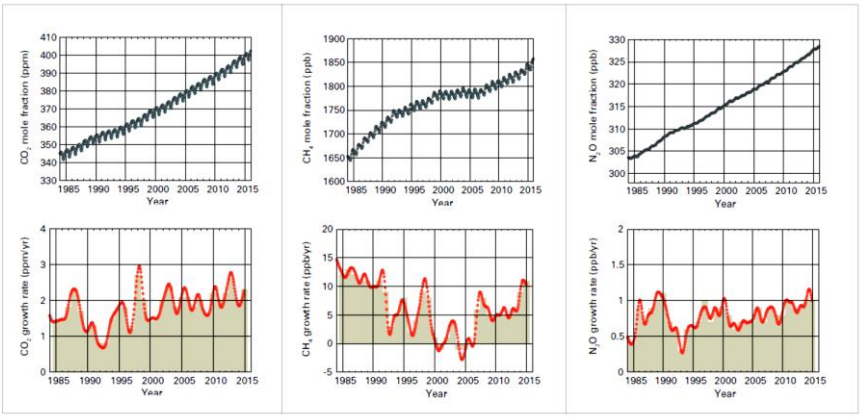

72. Measurements of CO2 in the atmosphere and in ice-trapped air show that GHGs have increased by about 40 per cent since 1800, with most of the increase occurring since the 1970s when global energy consumption accelerated (EEA, 2015a). Ice core data and other evidence suggest that current CO2 concentrations are higher than at any time in at least the last 2 million years years (Fig. 26), with the 400 ppm milestone reached in 09/05/2013 (NOAA, 2015).

73. Despite some climate mitigation measures, total global GHG emissions have increased continuously in recent decades (Figs. 26 and 27). Since 2014, CO2 and N2O concentration had growth rates slightly higher than the 1995-2014 average. CH4 concentration also showed growth, following a period of little change in 1999-2006 (NOAA, 2015; WMO, 2016). It has been estimated that approximately 44 per cent of the

total CO2 emitted by human activities might remain in the atmosphere, with the remaining 56 per cent stored in the oceans and the terrestrial biosphere (WMO, 2014, 2016).

Figure 26

Reconstruction of atmospheric CO2 over the past 55 million years based on proxy data (boron isotopes-blue circles, alkenones-black triangles and leaf stomata-green diamonds). Direct measurements from the past 800,000 years from Antarctic ice cores and modern instruments-pink. Future estimates are for the IPCC Representative Concentration Pathways (RCPs) 8.5 (red), 6 (orange), 4.5 (light blue) and 2.6 blue. Key: CE, Current Era (WMO, 2018).

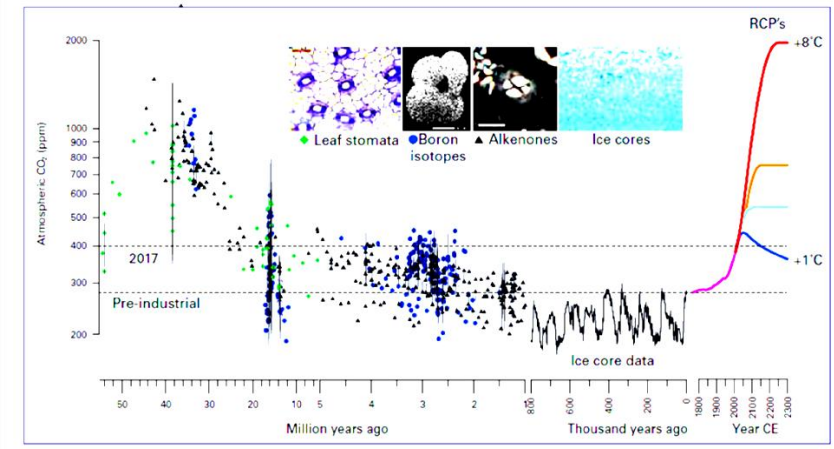

74. In addition, there appears to be a good correlation between the CO2 concentration and heat storage in the ocean (Fig. 27), which also presents an increasing problem for the coastal communities and infrastructure due to the documented relationship between ocean heat storage and SLR.

Figure 27

Evolution of ocean heat content (to 2000 m depth) and of the atmospheric carbon dioxide concentration (Source L. Cheng).

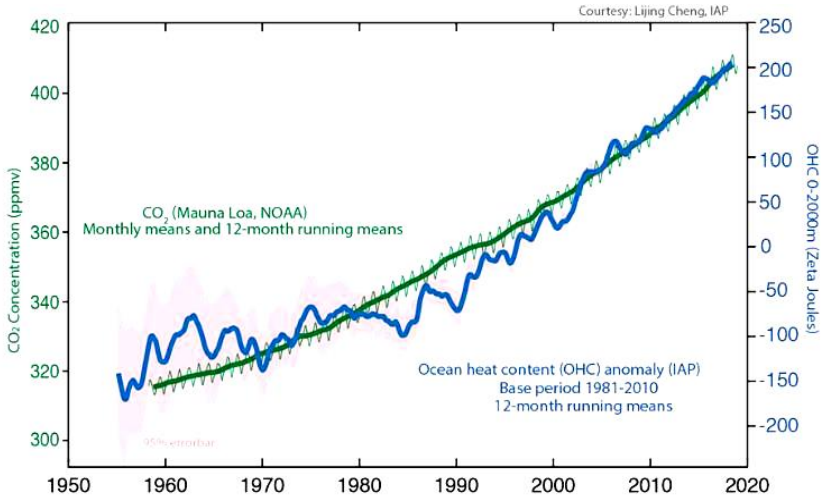

75. Breakdown of the total anthropogenic GHG emissions for 2010 revealed that CO2 accounted for 76 per cent (65 per cent due to fossil fuel combustion/industry and 11per cent due to land-use), CH4 for 16 per cent, N2O for 6 per cent and fluorinated gases for 2per

cent of the emissions (IPCC, 2014). Analysis of the total CO2 emissions from combustion for the period 1971–2010 showed that the primary drivers of the increasing trend are population growth and patterns of consumption/production (IPCC, 2014). Assessment of the CO2 emissions in relation to country income shows that these doubled for upper-mid-income countries (e.g. China and South Africa) for the period 1990–2010, almost reaching the level of high-income countries. A notable increase of CO2 emissions was also found in lower-mid-income countries (IPCC, 2014).

C. References

Alfieri L., Feyen L., Dottori F. and Bianchi A., 2015. Ensemble flood risk assessment in Europe under high end climate scenarios. Global Environmental Change 35,199-212. (doi:10.1016/j.gloenvcha.2015.09.004)

Alfieri L., Dottori F., Betts R., Salamon P., Feyen L., 2018. Multi-model projections of river flood risk in Europe under global warming. Climate 6, 16 doi:10.3390/cli6010016

AMAP, 2012. Arctic Climate Issues 2011: Changes in Arctic Snow, Water, Ice and Permafrost. SWIPA 2011.Overview Report

Androulidakis Y.S., Kombiadou K.D., Makris C.H., Baltikas V.N. and Krestenitis Y.N. 2015 Storm surges in the Mediterranean Sea: Variability and trends under future climatic conditions. Dynamics of Atmospheres and Oceans 71, 56–82.

Arnell N. et al 2014. Global-scale climate impact functions: the relationship between climate forcing and impact. Climate Change (134), 475–87.

Asariotis R., Mohos-Naray V., Benamara H., 2017. Port Industry Survey on Climate Change Impacts and Adaptation. UNCTAD Research Paper No. 18, UNCTAD/SER.RP/2017/18. 37 pp plus Appendices.

https://unctad.org/en/PublicationsLibrary/ser-rp-2017d18_en.pdf

Becker A., Acciaro A., Asariotis R., Cabrera E. et al., 2013. A note on climate change adaptation for seaports: A challenge for global ports, a challenge for global society. Climatic Change, 120, 683-695.

Beniston M. and Diaz H.F. 2004. The 2003 heat wave as an example of summers in a greenhouse climate? Observations and climate model simulations for Basel, Switzerland. Global and Planetary Change 44, 73–81.

Bertin X., Prouteau E. and Letetrel C. 2013. A significant increase in wave height in the North Atlantic Ocean over the 20th century. Global and Planetary Change 106, 77–83.

Camus P., Losada I.J., Izaguirre C., Espejo A., Menéndez M., Pérez J., 2017. Statistical wave climate projections for coastal impact assessments. Earth's Future 5, 918–933. https://doi.org/10.1002/2017EF000609

Canadell J.G., Le Quere C., Raupach M.R. et al. 2007. Contributions to accelerating atmospheric CO2 growth from economic activity, carbon intensity, and efficiency of natural sinks. Proceedings of the National Academy of Sciences 104, 18866-18870.

Carson M., Kohl A., Stammer D. et al., 2016. Coastal sea level changes, observed and projected during the 20th and 21st century. Climatic Change 134, 269-281. (doi: 10.1007/s10584-015-1520-1).

Cheng L., Abraham J., Hausfather Z., Trenberth K.E., 2019a. How fast are the oceans warming? Observational records of ocean heat content show that ocean warming is accelerating. Science 363 (6423), 128–129.

Cheng L., Zhu J., Abraham J. et al., 2019b. Continues Record Global Ocean Warming. Advances in Atmospheric Sciences 36 (3), 249–252. doi.org/10.1007/s00376-019-8276-x.

Church J.A., Clark P.U., Cazenave A., et al., 2013. Sea level change. In Climate Change 2013: The Physical Science Basis. Contribution of Working Group I to the Fifth Assessment Report of the Intergovernmental Panel on Climate Change. (T.F. Stocker, Qin D., Plattner G.-K. et al. [eds]) Cambridge; UK 1137–1216.

Conte, D. and Lionello, P. 2014. Storm Surge Distribution Along the Mediterranean Coast: Characteristics and Evolution, Procedia -Social and Behavioral Sciences 120, 110–115. (ISSN 1877-0428).

Coumou, D. and Rahmstorf, S. 2012. A decade of weather extremes. Nature Climate Change 29, 491-496. (doi:10.1038/nclimate1452).

Coumou D. and Robinson A., 2013. Historic and future increase in the global land area affected by monthly heat extremes. Environmental Research Letters 8 (3) iopscience.iop.org/article/10.1088/1748-9326/8/3/034018/meta.

Cowtan K. and Way R. G. 2014. Coverage bias in the HadCRUT4 temperature series and its impact on recent temperature trends. Q.J.R. Meteorol. Soc. 140, 1935–1944. (doi: 10.1002/qj.2297)

Cronin T.M., 2012. Rapid sea-level rise. Quaternary Science Reviews 56, 11–30.

Dai A., 2013. Increasing drought under global warming in observations and models. Nature Climate Change 3, 52–58.

De Conto R.M. and Pollard D., 2016. Contribution of Antarctica to past and future sea-level rise. Nature 531, 591-596. (doi: 10.1038/nature17145)

Dieng H.B., A. Cazenave, B. Meyssignac, K. von Schuckmanc and H. Palanisamya, 2017a. Sea and land surface temperatures, ocean heat content, Earth's energy imbalance and net radiative forcing over the recent years. Int. J. Climatol. (2017), 12 pp., doi: 10.1002/joc.4996

Dieng H. et al., 2017b. New estimate of the current rate of sea level rise from a sea level budget approach. Geophysical Research Letters, 44, doi: 10 .1002/ 2017GL073308.

Dole et al., 2011. Was there a basis for anticipating the 2010 Russian heat wave? Geophysical Research Letters 38, L06702.

Dutton A., Carlson A.E. , Long A. J. et al., 2015. Sea-level rise due to polar ice-sheet mass loss during past warm periods. Science 349, 6244 https://marine.rutgers.edu/pubs/private/Science-2015-Dutton-.pdf

ECE, 2013. Climate Change Impacts and Adaptation for International Transport Networks, United Nations Economic Commission for Europe, New York and Geneva, 2013, 248 pp. www.unece.org/fileadmin/DAM/trans/main/wp5/publications/climate_change_2014.pdf

EEA, 2010. The European environment: State and outlook 2010, Adapting to climate change. European Environmental Agency, Copenhagen. (ISBN 978-92-9213-159-3).

EEA, 2012. Climate change, impacts and vulnerability in Europe 2012. An indicator-based report. European Environmental Agency (EEA), Copenhagen, Denmark, 300 pp. (ISBN 978-92-9213-346-7)

EEA, 2014a. Projected changes in annual, summer and winter temperature. [Online image]. European Environment Agency (EEA). Available from: www.eea.europa.eu/data-and-maps/figures/projected-changes-in-annual-summer-1 [Accessed 01/03/2016].

EEA, 2014b. Trend in absolute sea level in European Seas based on satellite measurements (1992–2013). [Online image]. European Environment Agency (EEA). Available from: www.eea.europa.eu/data-and-maps/figures/sea-level-changes-in-europe-october-1992-may-1 [Accessed 01/03/2016].

EEA, 2014c. Projected change in relative sea level. [Online image]. European Environment Agency (EEA). Available from: www.eea.europa.eu/data-and-maps/figures/projected-change-in-sea-level [Accessed 01/03/2016].

EEA, 2015a, Global megatrends assessment: Extended background analysis complementing the SOER 2015 'Assessment of global megatrends'. European Environmental Agency, Copenhagen. (ISSN 1725-2237).

EEA, 2015b. Number of extreme heat waves in future climates under two different climate forcing scenarios. Available from: www.eea.europa.eu/data-and-maps/figures/number-of-extreme-heat-waves [Accessed 13/07/2015].

EEA, 2015c. Projected changes in heavy precipitation (in per cent) in winter and summer from 1971–2000 to 2071–2100 for the RCP8.5 scenario based on the ensemble mean of different regional climate models (RCMs) nested in different general circulation models (GCMs). Available from: www.eea.europa.eu/data-and-maps/figures/projected-changes-in-20-year-2 [accessed 21/03/2016].

Egorshev S., 2018. Presentation at the ECE Expert Group 18 and 19 December 2019, Geneva.a. www.unece.org/fileadmin/DAM/trans/doc/2018/wp5/2_Russian_Federation_Mr_Egorshev_Climate_Change_18-19_December_2018.pdf

Emanuel K. 2005. Increasing destructiveness of tropical cyclones over the past 30 years. Nature 436, 686-688.

EPA, 2015. Precipitation Worlwide, 1901-2013 [Online image]. Available from: https://www3.epa.gov/climatechange/science/indicators/weather-climate/precipitation.html [Accessed 03/02/2016].

Feyen L., Dankers R. and Bodis K., 2010. Climate warming and future flood risk in Europe. Climatic Change.

Forzieri G., Feyen L., Russo S. et al. 2016. Multi-hazard assessment in Europe under climate change. Climatic Change 137, 105 - 119. https://doi.org/10.1007/s10584-016-1661-x.

Fourier J. J., 1827. MEMOIRE sur les temperatures du globe terrestre et des espaces planetaires Memoires d l'Academie Royale des Sciences de l'Institute de France VII, pp. 570–60.

Fyfe J.C., Meehl G.A., England M.H. et al., 2016. Making sense of the early-2000s warming slowdown. Nature Climate Change 6, 224–228, doi:10.1038/nclimate2938.

Grinsted A., Moore J.C. and Jervejeva S., 2010. Reconstructing sea level from paleo and projected temperatures 200 to 2100 AD. Climate Dynamics 34, 461–472.

Hallegatte S., Green C., Nicholls R. J. and Corfee-Morlot J., 2013. Future flood losses in major coastal cities,Nature Climate Change 3, 802–806. (doi:10.1038/NCLIMATE1979)

Hanna E. et al., 2013. Ice sheet mass balance and climate change. Nature 498, 51–59.

Hansen J., Sato M., Hearty P. et al., 2016. Ice melt, sea level rise and superstorms: Evidence from paleoclimate data, climate modeling, and modern observations that 2°C global warming could be dangerous. Atmos. Chem. Phys. 16, 3761-3812 (doi:10.5194/acp-16-3761-2016).

Hay C.C., Morrow E., Kopp R.E. and Mitrovica J.X., 2015. Probabilistic reanalysis of twentieth-century sea-level rise. Nature 517, 481–484.

Hinkel J., Lincke D., Vafeidis A.T. et al., 2014. Coastal flood damages and adaptation costs under 21st century sea-level rise, Proceedings of the National Academy of Sciences USA, 111, 3292–3297.

Horton R., Herweijer C, Rosenzweig C, Liu J, Gornitz V, and Ruane AC, 2008. Sea level rise projections for current generation CGCMs based on the semi-empirical method. Geophysical Research Letters 35 DOI:10/1029/2007GL032486.

Horton, B.P., Rahmstorf, S., Engelhart, S.E. and Kemp, A.C. 2014. Expert assessment of sea-level rise by AD 2100 and AD 2300. Quaternary Science Reviews, 84, 1–6.

IPCC, 2007. Climate Change 2007. The Physical Science Basis. Contribution of Working Group I to the Fourth Assessment Report of the Intergovernmental Panel on Climate Change (Solomon S, D Qin, M Manning, Z Chen, M Marquis, KB Averyt, M Tignor and HL Miller (eds)). Cambridge University Press, Cambridge, UK and New York, NY, USA, 996 pp.

IPCC, 2013. Climate Change 2013: The Physical Science Basis. Contribution of Working Group I to the Fifth Assessment Report of the Intergovernmental Panel on Climate Change [Stocker T.F., Qin D., Plattner G.-K. et al. (eds.)]. Cambridge University Press, Cambridge, United Kingdom and New York, NY, USA.

IPCC, 2014. Summary for policy makers. In: Climate Change 2014: Impacts, Adaptation, and Vulnerability. Part A: Global and Sectoral Aspects. Contribution of Working Group II to the Fifth Assessment Report of the Intergovernmental Panel on Climate Change [Field C.B.,. Barros V.R Dokken D.J., et al. (eds.)]. Cambridge University Press, Cambridge, United Kingdom and New York, NY, USA, pp. 1-32.

IPCC, 2018: Summary for Policymakers. In: Global warming of 1.5°C. An IPCC Special Report on the impacts of global warming of 1.5°C above pre-industrial levels and related global greenhouse gas emission pathways, in the context of strengthening the global response to the threat of climate change, sustainable development, and efforts to eradicate poverty [V. Masson-Delmotte V., Zhai P., Pörtner J.O. et al. (eds.)]. World Meteorological Organization, Geneva, Switzerland 32 pp. www.ipcc.ch/site/assets/uploads/sites/2/2018/07/SR15_SPM_High_Res.pdf

IPCC SREX, 2012. Managing the Risks of Extreme Events and Disasters to Advance Climate Change Adaptation [Field C.B., Barros V., Stocker T.F. et al. (eds.)]. A Special Report of Working Groups I and II of the Intergovernmental Panel on Climate Change (IPCC). Cambridge University Press, Cambridge, UK, and New York, NY, USA. 582 pp.

Jevrejeva S., Moore J.C. and Grinsted A., 2010. How will sea level respond to changes in natural and anthropogenic forcings by 2100? Geophysical Research Letters 37. DOI: 10.1029/2010GL042947.

Jevrejeva S., Moore J.C. and Grinsted A. 2012. Sea level projections to AD2500 with a new generation of climate change scenarios. Global and Planetary Change 80–81, 14–20. (doi:10.1016/j.gloplacha.2011.09.006).

Jevrejeva S., Jackson L.P., Riva R.E.M., Grinsted A., Moore J.C., 2016. Coastal sea level rise with warming above 2°C. Proc. Natl. Acad. Sci. 113, 13342 LP-13347. https://doi.org/10.1073/pnas.1605312113.

Karl T.R., Melillo J. T. and Peterson T. C. 2009. Global Climate Change Impacts in the United States. Cambridge University Press, 189 pp.

Karl T.R., Arguez A., Huang, B. et al., 2015. Possible artifacts of data biases in the recent global surface warming hiatus, Science, 348, pp. 1469–1472.

Katsman C.A., Sterl A., Beersma J.J. et al., 2011. Exploring high end scenarios for local sea level rise to develop flood protection strategies for a low-lying delta. The Netherlands as an example. Climatic Change 109 (3-4), 617–645. (doi:10.1007/s10584-011-00375)

King D., Schrag D., Dadi Z., Ye Q. and Ghosh A. 2015. Climate Change: A Risk Assessment. Centre for Science and Policy, University of Cambridge. (www.csap.cam.ac.uk/media/uploads/files/1/climate-change--a-risk-assessment-v9-spreads.pdf)

Kopp R., Simons F., Mitrovica J., Maloof A. and Oppenheimer M., 2009. Probabilistic assessment of sea levelduring the last interglacial stage. Nature 462, 863–867. (doi:10.1038/nature08686).

Lionello P., Galati M.B. and Elvini E. 2012. Extreme storm surge and wind wave climate scenario simulations at the Venetian littoral. Phys Chem Earth Parts A/B/C 40–41, 86–92.

Losada I.J., Reguero B.J., Mendez F.G., et al., R. 2013. Long-term changes in sea level components in Latin America and the Caribbean. Global and Planetary Change 104, 34–50.

Marcos M., Jorda G., Gomis D. and Perez B. 2011. Changes in storm surges in southern Europe from a regional model under climate change scenarios. Global and Planetary Change 77(3–4), 116–128. (doi:10.1016/j.gloplacha.2011.04.002)

Mel R., Sterl A. and Lionello P. 2013. High resolution climate projection of storm surge at the Venetian coast. Nat Hazards Earth System Science 13, 1135–1142.

Menendez M. and Woodworth P.L. 2010. Changes in extreme high water levels based on a quasi-global tidegauge data set. Journal of Geophysical Research, 115, C10011. (doi:10.1029/2009JC005997).

Menounos, B., Hugonnet R., Shean D. et al., 2018. Heterogeneous Changes in western North American glaciers linked to decadal variability in zonal wind strength. Geophysical Research Letters 45, https://doi.org/10.1029/2018GL08094.

Mentaschi L., M. I. Vousdoukas E. Voukouvalas A. Dosio, and L. Feyen, 2017. Global changes of extreme coastal wave energy fluxes triggered by intensified teleconnection patterns. Geophys. Res. Let. 44, 2416–2426, doi:10.1002/2016GL072488.

MetOffice, 2014. Climate risk An update on the science. Met Office, Handley Center, Devon, UK, 9 pp.

Meyer-Christoffer A., Becker A., Finger P. et al., 2015. GPCC Climatology Version 2015 at 0.25◦: Monthly Land-Surface Precipitation Climatology for Every Month and the Total Year from Rain-Gauges Built on GTS-Based and Historic Data; GPCC: Offenbach, Germany, 2015.

Milly P.C.D., Betancourt J., Falkenmark M. et al., 2008. Stationarity is dead: Whither water management? Science 319, 573–574.

Monioudi I. N., Asariotis R. Becker A. et al., 2018. Climate change impacts on critical international transportation assets of Caribbean Small Island Developing States (SIDS): The case of Jamaica and Saint Lucia. Regional Environmental Change, 18 (8), 2211–2225.

Mora C., Dousset B., Caldwell I.R. et al., 2017. Global risk of deadly heat. Nature Climate Change 7, 501-507. DOI: 10.1038/NCLIMATE3322

Mori N., Shimura T., Yasuda T. and Mase H., 2013. Multi-model climate projections of ocean surface variables under different climate scenarios—Future change of waves, sea level and wind. Ocean Engineering, http://dx.doi.org/10.1016/j.oceaneng.2013.02.016i

Moss R. et al., 2010. The next generation of scenarios for climate change research and assessment. Nature 463, 747–756.

Munich Re, 2015. NatCatSERVICE: Loss events worldwide 1980–2014.

NASA, 2016. NOAA Analyses Reveal Record-Shattering Global Warm Temperatures in 2015 [WWW] Goddard Institute for Space Studies. Available from: www.giss.nasa.gov/research/news/20160120/ [Accessed 13/02/2016]

NOAA, 2015. 2014 State of the Climate: Carbon Dioxide [WWW] Available from: https://www.climate.gov/news-features/understanding-climate/2014-state-climate-carbon-dioxide

NOAA, 2016. Global Analysis - Annual 2015: 2015 year-to-date temperatures versus previous years [WWW] National Centers for Environmental Information. Available from: www.ncdc.noaa.gov/sotc/global/2015/13/supplemental/page-3 [Accessed 122/02/2016]

NOAA, 2017a. National Centers for Environmental Information (NCEI). 2016 Officially Warmest Year on Record. (Published online January 2017, accessed on May 24, 2017 www.nnvl.noaa.gov/MediaDetail2.php?MediaID=1989&MediaTypeID=3&ResourceID=105007/

NOAA, 2017b. National Center for Environmental Information (NCEI), State of the Climate: Global Snow and Ice for 2016. (Published online 01/2017, retrieved on May 9, 2017 from www.ncdc.noaa.gov/sotc/global-snow/201613

NOAA, 2017c. National Centers for Environmental Information (NCEI) U.S. Billion-Dollar Weather and Climate Disasters. www.ncdc.noaa.gov/billions/

NSIDC, 2017. National Snow and Ice Data Center. Snow, Ice and Climate Change (retrieved on May 24, 2017 from nsidc.org/cryosphere/climate-change.html

Pérez J., Menendez M., Mendez F. and Losada I. 2014. Evaluating the performance of CMIP3 and CMIP5 global climate models over the north-east Atlantic region. Climate Dynamics 43, 2663–2680.

Pfeffer W., Harper J. and O' Neel S., 2008. Kinematic constraints on glacier contributions to 21st century sea level rise. Science 321, 1340–1343. (doi:10.1126/science.1159099).

Rahmstorf S., Cazenave A., Church J.A. et al., 2007. Recent climate observations compared to projections. Science 316, 709–709.

Rahmstorf S., 2012. Climate Change: State of Science . In: Maritime Transport and the Climate Change Challenge, R. Asariotis and H. Benamara, eds., Earthscan, pp. 3–11.

Rahmstorf S., Foster G., Cahill N., 2017. Global temperature evolution: recent trends and some pitfalls. Environmental Research Letters 12, 054001.

Ranasinghe R., 2016. Assessing climate change impacts on open sandy coasts: A review. Earth Science Reviews 160, 320-332.

Richardson K., Steffen W., Schellnhuber H.J. et al., 2009. Synthesis Report. Climate change: Global Risks, Challenges and Decisions. University of Copenhagen, 39 pp.

Rignot, E., Velicogna, I., van den Broeke, M.R., Monagha, A. and Lenaerts, J. 2011. Acceleration of the contribution of the Greenland and Antarctic ice sheets to sea level rise. Geophysical Research Letters, (38), 5 pp. (doi:10.1029/2011GL046583).

Rignot E., Mouginot, J., Scheuchl, B. et al., 2019. Four decades of Antarctic Ice Sheet mass balance from 1979–2017. PNAS doi.org/10.1073/pnas.1812883116

Rohling E., Grant K., Hemleben C. et al., 2008. High rates of sea level rise during the last interglacial period. Nature Geosciences 1, 38–42. (doi:10.1038/ngeo.2007.28).

Rueda A., Vitousek S., Camus P. et al., 2017. A global classification of coastal flood hazard climates associated with large-scale oceanographic forcing. Scientific Reports 7, 5038. doi.org/10.1038/s41598-017-05090-w

Ruggiero P., Komar P.D. and Allan J.C., 2010. Increasing wave heights and extreme value projections: The wave climate of the U.S. Pacific Northwest. Coastal Engineering 57, 539–552.

Ruggiero P. 2013. Is the intensifying wave climate of the U.S. Pacific Northwest increasing flooding and erosion risk faster than sea-level rise? Journal of Waterway, Port, Coastal, and Ocean Engineering 139 (2), 88–97.

Schneider U., Finger P., Meyer-Christoffer A., 2017. Evaluating the Hydrological Cycle over Land Using the Newly-Corrected Precipitation Climatology from the Global Precipitation Climatology Centre (GPCC). Atmosphere ,8 (52), doi: 10.3390/atmos8030052.

Schuur EAG, McGuire A.D., Schädel C., et al., 2015. Climate change and the permafrost carbon feedback. Nature 520, 171–179. 10.1038/nature14338

Seneviratne, S. I., et al., 2016. Allowable CO2 emissions based on regional and impact-related climate targets. Nature 529, 477–483. doi:10.1038/nature16542.

Shakun J.D., Clark P.U., He F. et al., 2012. Global warming preceded by increasing carbon dioxide concentrations during the last deglaciation, Nature 484, 49–55.

Simmons A.J., P. Berrisford, D.P. Dee, H. Hersbach, S. Hirahara and J.N. Thepaut, 2017. A reassessment of temperature variations and trends from global reanalyses and monthly surface climatological datasets. Q.J.R. Meteorol. Soc. 143, 101–119, doi:10.1002/qj.2949.

Steffen, W. 2009. Climate Change 2009: Faster Change and More Serious Risks. Report to the Department of Climate Change, Australian Government.

Taalas P., 2019. WMO presentation, UN Oceans Meeting, 7–8 February 2019, Geneva.

Trenberth K.E., Cheng L., Jacobs P., Zhang Y., Fasullo J.T., 2018. Hurricane Harvey links to ocean heat content and climate change adaptation. Earth's Future 6, 730–744. doi.org/10.1029/2018EF000825

U.S. Climate Resilience Toolkit, 2015. Arctic Development and Transport. [WWW] Available from: toolkit.climate.gov/content/about-climate-resilience-toolkit (accessed 15/01/2016).

UNFCCC, 2015. The Paris Agreement by Parties to the United Nations Framework Convention on Climate Change. unfccc.int/meetings/paris_nov_2015/items/9445.php.

Van der Wiel K., Kapnick S.B. and Vecchi G.A., 2017. Shifting patterns of mild weather in response to projected radiative forcing. Climatic Change 140, 649-658. doi: 10.1007/s10584-016-1885-9.

Velicogna I., Sutterley T. C. and van den Broeke M. R. 2014. Regional acceleration in ice mass loss from Greenland and Antarctica using GRACE time-variable gravity data. Geophys. Res. Lett., 41(22), 8130-8137.

Vellinga P. et al. 2008. Exploring high-end climate change scenarios for flood protection of the Netherlands.International Scientific Assessment for the Delta Committee. SR WR-2009-05. KNMI, Alterra, The Netherlands. www.knmi.nl/bibliotheek/knmipubWR/WR2009-05.pdf.

Vermeer M. and Rahmstorf S., 2009 Global sea level linked to global temperature. Proceedings of the National Aceademy of Sciences USA 106, 21527–21532. (doi:10.1073/pnas.0907765106).

Vogel M.M., R. Orth, F. Cheruy , S. Hagemann , R. Lorenz, B.J.J.M. van den Hurk, and S.I. Seneviratne, 2017. Regional amplification of projected changes in extreme temperatures strongly controlled by soil moisturetemperature feedbacks. Geophys. Res. Letters, 44, 1511–1519. doi:10.1002/ 2016GL071235.

Vousdoukas M.I., Voukouvalas E., Annunziato A., Giardino A. and Feyen, L., 2016a. Projections of extreme storm surge levels along Europe. Climate Dynamics doi: 10.1007/s00382-016-3019-5.

Vousdoukas M.I., E. Voukouvalas, L. Mentaschi, F. Dottori, A. Giardino, D. Bouziotas, A. Bianchi, P. Salamon and L. Feyen, 2016b. Developments in large-scale coastal flood hazard mapping. Nat. Hazards Earth Syst. Sci. 16, 1841–1853, doi:10.5194/nhess-16-1841-2016.

Vousdoukas M.I., L. Mentaschi, E. Voukouvalas, M. Verlaan, and L. Feyen, 2017. Extreme sea levels on the rise along Europe's coasts. Earth's Future 5, 304–323. doi:10.1002/2016EF000505.

Vousdoukas M.I., Mentaschi L., Voukouvalas E., Verlaan M., Jevrejeva S., Jackson L.P., Feyen L., 2018. Global probabilistic projections of extreme sea levels show intensification of coastal flood hazard. Nat. Commun. 9, 2360. doi.org/10.1038/s41467-018-04692-w.

Wada Y., van Beek L.P.H., Weiland F.C.S. et al., 2012. Past and future contribution of global groundwater depletion to sea-level rise. Geophys Res Letters 39, L09402. (doi: 10.1029/2012GL051230)

Wester, P., Mishra, A. Mukherji, A. Shrestha. A.B., (eds), 2019. The Hindu Kush Himalaya Assessment- Mountains, Climate Change, Sustainability and People. Springer Nature Switzerland AG, Cham. link.springer.com/content/pdf/10.1007per cent2F978-3-319-92288-1.pdf

WMO, 2014. Statement on the status of the global climate in 2014, World Meteorological Organization, WMO-No. 1152, Chairperson, Publications Board, Geneva, 22 pp. (ISBN: 978-92-63-11152-4.)

WMO, 2016. WMO Statement on the Status of the Global Climate in 2015, World Meteorological Organization, WMO-No. 1167, Chairperson, Publications Board, Geneva, Switzerland, 26 pp. (ISBN: 978-92-63-11167-8.). See also www.indiaenvironmentportal.org.in/content/421694/provisional-statement-on-the-status-of-global-climate-in-2011-2015/.

WMO, 2017. WMO Statement on the State of the Global Climate in 2016. World Meteorological Organization Report 1189, library.wmo.int/opac/doc_num.php?explnum_id=3414).

WMO, 2018. WMO Statement on the State of the Global Climate in 2017. World Meteorological Organization Report 1212. library.wmo.int/doc_num.php?explnum_id=4453.

Yan X.-H., Boyer T., Trenberth K. et al., 2016. The global warming hiatus: Slowdown or redistribution? Earth's Future, 4, 472–482, doi:10.1002/2016EF000417.